Mobility of charges in liquid, solid, and dense gaseous helium

V. B. Shikin

Institute of Solid State Physics, USSR Academy of Sciences, Chernogolovka
Usp. Fiz. Nauk **121**, 457–497 (March 1977)

The aim of this review is to provide a systematic survey of the extensive experimental and theoretical data obtained recently as a result of studies of the motion of charged particles in liquid, solid, and gaseous helium. The great variety of the available material has forced a subdivision of the general question of the motion of charged particles in helium into a number of "autonomous" areas. The motion of charges in a homogeneous medium at sufficiently low velocities is discussed. Chapter 1 describes the structure of positive (cations) and negative (anions) helium ions in liquid helium. It is noted that there is good agreement between theoretical descriptions and observed characteristics of ions in helium. The nucleation of electron bubbles in dense gaseous helium is investigated. Chapter 2 surveys theoretical and experimental results on the mobility of helium ions under kinetic conditions. The structure of helium ions ensures that the ion scattering cross sections of different thermal and impurity excitations exhibit very varied properties. Each of the basic scattering mechanisms, i.e., the phonon mechanism, scattering of impurities in weak He^3-He^4 solutions, the Fermi-fluid mechanism, and the roton mechanism, which are listed here in order of increasing complexity of interpretation, must therefore be specially considered. There have been notable successes in the theoretical interpretation of the kinetic mobility of helium ions, but there are also the characteristic difficulties which impede the development of a complete theory of the kinetic mobility of helium ions. Chapter 3 reviews the results obtained as a result of studies of the mobility of helium ions when the hydrodynamic approximation can be used in dense gaseous and in solid helium.

PACS numbers: 66.10.Ed, 67.80.Mg, 67.40.Pm, 51.20.+d

CONTENTS

INTRODUCTION

The introduction of a charged particle into dense helium[1)] (solid, liquid, or gaseous) leads to the formation of various elaborate complexes consisting of the charged particle proper and the ambient helium interacting with the charge. The large number of effects involving the participation of these complexes, which are often called helium ions, the excellent experimental possibilities, and the relatively lucid interpretation of the most important observable facts have stimulated the publication of a large number of papers, both experimental and theoretical, and this has resulted in the development of a new field of research in helium physics in a relatively short time (say, the last fifteen to twenty years).

Originally, most of the research effort was directed toward the determination of the structure of the helium ion. The work of Williams, Shal'nikov, Meyer, Reif, Atkins, Ferrel, Careri, Rayfield, and others, has ensured that the structure of helium ions in liquid helium is now practically completely established. The results obtained by these researchers in the case of charges in homogeneous helium is considered in the first part of this review.

Another and much more extensive range of problems arises in the interpretation of the experimental data on the mobility of helium ions under different special conditions as a function of temperature, guiding field, concentration of impurity excitations, and so on. It is important to note that the mobility of charged particles is the most readily measured characteristic of such ions. It follows that our understanding of the properties of helium ions is, in many ways, determined by the current state of the theory of the mobility of such ions. Moreover, by observing the behavior of ions in helium and by being able to explain this behavior, it is, as a rule, possible to extract from the mobility data, a considerable amount of interesting information on the properties of liquid helium itself. The second part of this review gives a description of the simpler dynamic properties of helium ions moving slowly through a homogeneous medium under the action of a weak electric field.

Studies of the thermal properties of liquid helium itself and quantitative interpretation of experimental data on the mobility of helium ions are possible only in cer-

[1)]The methods used to introduce the ions into helium, and to measure their mobility, are analogous to the classical methods for studying the mobility of ions in gases (see, for example, the review by Smirnov[20]).

tain temperature intervals. These intervals are as follows:

a) the low-temperature region with well-defined concepts of thermal and impurity excitations, and an excitation path length l greater than the ionic radius $R(l > R)$;

b) the hydrodynamic region in which $l < R$;

c) the neighborhood of the λ point.

In addition, the mobility of charges in dense gaseous and solid helium also deserves attention.

In view of the considerable volume of data on helium-ion mobility, it will be convenient to subdivide the second part into two chapters. One will consider the mobility of charges under kinetic conditions, and the other will summarize existing information on other types of mobility.

1. STRUCTURE OF HELIUM IONS

At least three qualitatively different ionic complexes are observed in homogeneous helium: positive ions, negative ions, and charged vortex rings. In addition, independent ionic formations may also be considered to include charged surface states existing near the liquid-vapor interface of liquid helium. The great variety of possibilities forces us to subdivide the general problem of helium ions into a number of "autonomous" areas. They are defined in the introduction. Throughout this review, we confine our attention to the mobility of ions in a homogeneous medium at low velocities. Under such conditions, only the positive and negative ions need be defined.

A. Positive ions (cations)

Positive ions, or cations, in liquid helium are usually defined as charged particles with a bare mass of the order of the mass of the helium atom. Any description of the properties of such particles in liquid helium must take into account the polarization interaction between the charge and the ambient helium. This point was first noted by Atkins[1] and enabled him to put forward a simple model of a cation in the form of a charge surrounded by a sphere of solidified helium. The radius of the sphere can be estimated as follows. The electric field $E = e/R^2$ of a point charge produces in the ambient liquid an excess pressure P_α of polarization origin, which is given by

$$P_\alpha = \frac{\alpha e^2}{2v_4 r^4}, \quad r > a, \tag{1.1}$$

i.e., it is inversely proportional to the fourth power of the distance (α is the atomic polarizability, v_4 is the effective volume per atom of the liquid, r is the distance from the center of the ion, and a is the interatomic distance).

If we take into account the fact that liquid helium solidifies under a pressure $P_s \approx 25$ atm, and if we set $P_\alpha(r) = P_s$, we find that the solidification radius R_+ is given by

$$R_+^4 = \frac{\alpha e^2}{2v_4 P_s}. \tag{1.2}$$

This macroscopic definition of the radius R_+ is meaningful if $R_+ \gg a$. Numerical estimates of R_+, obtained for $\alpha = 5 \times 10^{-25}$ cm^3 and $v_4 \approx a^3$ yield $R_+ \approx 6$–7 Å for $a \approx 3.5$ Å. In other words, the inequality $R_+ > a$ is, in fact, satisfied but with a small margin.

The effective mass M_+ of a cation in the Atkins model consists of the mass of the solid nucleus of radius R_+, the mass of the excess-density liquid around the nucleus, and the attached mass. This means that M_+ is roughly, $60m_{He^4}$–$80m_{He^4}$. The particular feature of liquid helium is that, because of the low solidification pressure, even small polarizability is sufficient in the above model to result in the formation of a quasimacroscopic helium-solidification region around the positive charge. This, in turn, gives rise to a sharp increase in the effective cation mass and a reduction in its mobility.

The simplicity and ease of physical interpretation of the Atkins model were such that all subsequent publications on the observed properties of the cations involved attempts to explain these data in terms of the solid sphere model. The most complete account of the corresponding theory is given in Arkhipov's review.[2] However, there is now a sufficient number of facts that cannot be fitted into the framework of the Atkins model and require a more rigorous inclusion of the interaction between charges and liquid helium. Examples of this kind of discrepancy are discussed below. Nevertheless, Atkins' model retains its significance as the first approximation which can be used to estimate the scale of the various effects.

In a more rigorous description of the properties of a cation, the two most important characteristics are the excess pressure P_α (1.1) and the experimentally measured effective mass M_+.[2)] The resonance method of measuring M_+[4,5][3)] yields the value

---

[2)] A rigorous theoretical calculation of M_+ has not as yet been made although some attempts at this have been published.[3]

[3)] Helium ions located near the vapor-liquid boundary are repelled from it by the electrostatic image force

$$F = \left(\frac{e}{2x}\right)^2 \frac{\varepsilon - 1}{\varepsilon(\varepsilon + 1)}; \tag{*}$$

where x is the distance of the ion from the surface, ε is the dielectric constant $\varepsilon - 1 = 0.06$ of the liquid ($\varepsilon \approx 1$ for the gas), and $F > 0$ corresponds to repulsion. By equating this repulsive force to the external field $E_\perp$, which holds the ion on the surface, it is possible to fix the position of the ion at any given depth x_0 from the surface. This depth is given by

$$x_0 = \frac{1}{2}\sqrt{\frac{e}{E_\perp}\frac{\varepsilon - 1}{\varepsilon(\varepsilon + 1)}}. \tag{**}$$

This provides us with a very convenient means of observing a number of effects. In particular, the ions execute small natural oscillations around x_0[4] with a characteristic frequency ω_0 given by

$$\omega_0^2 = \frac{1}{2M_\pm}\frac{e^2(\varepsilon - 1)}{x_0^3(\varepsilon + 1)}, \tag{***}$$

where $M_\pm$ is the effective cation (anion) mass. Experimental determination of the frequency ω_0 yields direct information on the effective mass $M_\pm$. Such experiments have been carried out by Poitrenaud and Williams.[5] A typical resonance curve showing the absorption of high-frequency radiation by the ions is given in Fig. 1.

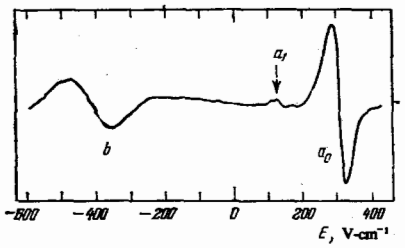

FIG. 1. Resonance lines for cations (a_0) and anions (b) at 208 MHz and $T = 0.7$ °K.[5] The first harmonic (a_1) is also seen in the case of cations. The external frequency were fixed in this experiment, and the natural frequencies of the ions were varied by varying the applied electric field (plotted along the ordinate axis).

$$M_+ = (45 \pm 2)\, m_{\mathrm{He}^4}, \tag{1.3}$$

which is substantially different from estimates of M_+ based on the Atkins model. Insofar as the radius R_+ is concerned, it does not play a universal role in the more rigorous theory and, in principle, need not be used at all.

B. Negative ions (anions)

The structure of negative ions produced in liquid helium when some light particle (for example, an electron—which is the most stable and readily available) is introduced into helium, has been found to be novel and in its time unexpected. Such particles produce bubbles in helium and are localized inside the spherical cavities.[6,7]

The formation of bubbles is made possible by a combination of several circumstances. Firstly, an individual helium atom is a stable quantum system and does not attach to itself a surplus electron at distances of the order of the Bohr orbit. A free electron introduced artificially into dense helium, and forced to move in the interatomic spaces between individual atoms that repel it, has therefore a high zero-point oscillation energy W_e. In the optical model, which is widely used at present to describe the interaction of electrons with dense helium, this energy is estimated from the following expression:

$$W_e = \frac{2\pi\hbar^2 a_0}{m_e} n, \tag{1.4}$$

where n is the density of helium, m_e is the electron mass, and a_0 is the effective scattering length for an electron on helium atoms. The numerical value of a_0 is chosen so that, at $n \approx 2\times10^{22}$ cm^{-3}, the energy W_e given by (1.4) is equal to the measured work done on introducing an electron into liquid helium ($W_e \approx 1.0$ eV).[8] Hence, it follows that $a_0 \approx 0.62$ Å. One other property of helium which facilitates the formation of bubbles is its low surface tension on the liquid-vapor interface. This ensures that the total energy W expended in forming the bubble can be simply estimated, and turns out to be much less than W_e, so that the electron is, in fact, conveniently localized and produces a bubble.

Estimates of the anion parameters, first carried out by Ferrel[6] and somewhat later by Carera, Fasoli, and Gaeta,[7] [4)] were quite elementary and, at the same time, sufficiently accurate because the resulting complex is quasimacroscopic (the formal condition for this is $m_e/m_{\mathrm{He}^4} \ll 1$). The basic idea is to minimize the total anion energy

$$W = \frac{\pi^2\hbar^2}{2m_e R^2} + 4\pi\sigma R^2$$

with respect to the radius R (m_e is the mass of the free electron and σ is the surface tension on the free helium surface). This yields

$$R_-^4 = \frac{\pi\hbar^2}{8m_e\sigma}, \tag{1.5}$$

so that the energy is given by

$$W = 4\pi\hbar\sqrt{\frac{\pi\sigma}{2m_e}}. \tag{1.5a}$$

For $\sigma = 0.36$ erg/cm^2, the numerical value of R_- in liquid He^4 turns out to be of the order of 18 Å. Equation (1.5a) then yields $W \approx 0.1$ eV, i.e., $W \ll W_e$ and the localization of the electron is, clearly, favored.

It is important to note that, under the usual conditions, when external pressure is zero, the polarization forces which play the dominant role in the formation of cations are in practice not perceptible during the formation of the bubble because the inequality $R_- \gg R_+$ is well satisfied.

If we neglect the polarization of helium around the anion, and recall that the electron mass is relatively small, we may conclude that the effective anion mass M_- must be equal to its associated hydrodynamic mass

$$M_- = \frac{2}{3}\pi R_-^3 \rho \tag{1.6}$$

(where ρ is the mass density of helium).

Resonance measurements yield the following result[5]:

$$M_- = (243 \pm 5)\, m_{\mathrm{He}^4}, \tag{1.6a}$$

and this corresponds to

$$R_- = (1.74 \pm 0.02)\cdot10^{-7} \text{ cm}. \tag{1.7}$$

The agreement between the theoretical (1.5) and experimental (1.7) values of R_- must be regarded as fully satisfactory. The agreement can, however, be improved

---

[4)] The possibility of formation by light particles (electrons, positrons, and so on) of localized states inside an empty bubble in helium was first noted by Ferrel[6] in connection with the properties of ortho- and parapositronium in liquid helium. However, a definitive demonstration of the existence of such bubbles become possible only after the introduction of light charged particles (electrons) into helium.[7] The appearance of charged bubbles has by now been observed in other nonpolar liquids, i.e., neon and hydrogen.[9a] It is interesting to note that the introduction of positrons into dense gaseous helium results in the appearance not of bubbles but of clusters.[9b]

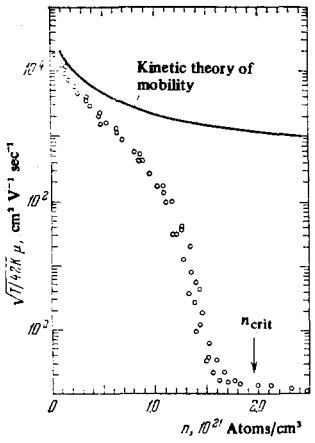

FIG. 2. Mobility of electrons in gaseous helium at $T = 4.2$ °K.[11] Arrow shows the calculated value of n_{crit}.

by solving the electron localization problem more carefully. This was done by Springett *et al.*,[10] who obtained a theoretical value for R_- equal to 17.0 Å.

C. Anions in gaseous and solid helium

1) In gaseous helium, it is possible to vary the density of the medium within very broad limits and thus investigate the development of electronic bound states. This possibility is beautifully illustrated by the experiments of Levin and Sanders,[11] who measured the mobility of free electrons in dense gaseous He^4. Figure 2 shows the data[11] on the mobility of electrons in a weak guiding field as a function of gas density. It is clear from this figure that the critical gas density which separates the regions of existence of strongly and weakly localized electronic states lies in the neighborhood of $n_{crit} \sim 10^{21}$ cm^{-3}. When the gas density is varied in this region by a factor of only three or four, the carrier mobility falls by roughly five orders of magnitude from a value which is in good agreement with calculations based on ordinary gas-kinetic theory for free electrons down to a value which is almost equal to the mobility of anions in liquid helium. This sharp reduction in mobility was justifiably interpreted by Levin and Sanders as being due to the onset of the formation of anions in dense gaseous helium.

Initially, the localized states are still quite "shallow" and are therefore very sensitive to the influence of various external fields. This means that, for the intermediate values of n, there is a range of electronic bound states which are qualitatively different from the bound states in the liquid.

The equations for the self-consistent bound states of an electron in gaseous helium can be obtained, as usual, by minimizing the free energy of the system. We shall suppose that the de Broglie wavelength of an electron is much greater than the mean separation between the helium atoms, so that the electron is in the mean field produced by the helium atoms which, in turn, is determined by their concentration $n(\mathbf{r})$. Moreover, it is interesting for future purposes to introduce a constant uniform magnetic field.

The contribution of the interaction between the electron and the gas to the free-energy density can be written by analogy with (1.4) in the form

$$\tilde{F}_{\text{int}} = \frac{2\pi\hbar^2 a_0}{m_e} n(\mathbf{r}) |\varphi(\mathbf{r})|^2, \tag{1.8}$$

where $a_0 = 0.62$ Å is the scattering length of electrons on helium atoms in the pseudopotential approximation, $\varphi(\mathbf{r})$ is the electron wave function, and m_e the electron mass. This means that, if we neglect the interaction between the helium atoms and suppose that the gas is classical, the free-energy density of the system in an external field with vector potential $\mathbf{A}(\mathbf{r})$ is given by

$$\tilde{F} = \frac{1}{2m_e}\left|\left(\hat{\mathbf{p}} + \frac{e}{c}\mathbf{A}\right)\varphi\right|^2 + \tilde{F}_{\text{int}} + nT\ln(nB), \tag{1.9}$$

where $B(T)$ is a known function of temperature.

By varying the free energy $F = \int_V \tilde{F}\,dV$ with respect to $n(\mathbf{r})$ and $\varphi(\mathbf{r})$ at constant volume V of the system and subject to the condition

$$\int |\varphi(\mathbf{r})|^2\,d\mathbf{V} = 1,$$

we have, as $V \to \infty$ and $N/V \to n_0$,

$$n(\mathbf{r}) = n_0 \exp\left(-\frac{\psi}{T}\right), \tag{1.10}$$

$$\psi = \frac{2\pi\hbar^2 a_0}{m_e}|\varphi(\mathbf{r})|^2, \tag{1.10a}$$

$$F = \int\left[\frac{1}{2m_e}\left|\left(\hat{\mathbf{p}} + \frac{e}{c}\mathbf{A}\right)\varphi\right|^2 + n_0 T\left(1 - e^{-\psi/T}\right)\right]d\mathbf{V} + n_0 T\ln(n_0 B). \tag{1.11}$$

The second term in (1.11) is the free energy of a perfect gas.

The normalized extremal $\varphi(r)$ of the functional (1.11) satisfies the equation

$$\frac{1}{2m_e}\left(\hat{\mathbf{p}} + \frac{e}{c}\mathbf{A}\right)^2\varphi + \frac{2\pi\hbar^2 a_0}{m_e} n(\mathbf{r})\varphi = \lambda\varphi. \tag{1.12}$$

In the absence of the magnetic field, the wave function of a localized electron is spherically symmetric and we shall assume, for simplicity, that

$$\varphi(\mathbf{r}) = \pi^{-1/2} k^{3/2} \exp(-kr).$$

The change in the free energy, $\delta F_0(k)$, due to the localization of the electron is given by

$$\delta F_0(k) = F_0(k) - n_0 T\ln(n_0 B) - \frac{2\pi\hbar^2 a_0 n_0}{m_e}$$

or, in terms of the dimensionless variables,

$$\varkappa = \frac{k}{k_0}, \quad \tilde{n} = \frac{n}{n^*}, \quad \delta F_0 = \frac{\delta F}{\varepsilon_0}, \qquad k_0^3 = \frac{m_e T}{2\hbar^2 a_0}, \quad n^* = \frac{1}{2\pi a_0}\left(\frac{m_e T}{2\hbar^2 a_0}\right)^{2/3}, \quad \varepsilon_0 = \frac{\hbar^2 k_0^2}{2m_e}, \tag{1.13}$$

we have[12]

$$\delta F_0(\varkappa) = \varkappa^2 + \tilde{n}\left[\frac{1}{3}\int_0^\infty s^3 e^{-s}\exp\left(-\varkappa^3 e^{-s}\right)ds - 2\right]. \tag{1.14}$$

Figure 3 (curves 1–5) shows graphs of $\delta F_0(\varkappa)$ obtained from (1.14) for different $\tilde{n}$. Electronic bound states which correspond to a negative minimum of $\delta F_0(\varkappa)$ ap-

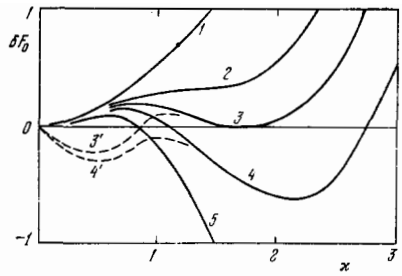

FIG. 3. δF_0 as a function of $\varkappa$ for different n. Curves 1–5 correspond, respectively, to $\tilde{n}=4$, 6, 7, 8, and 10. Dashed curves show δF_0 as a function of $\varkappa$ for small $\varkappa$. Curves 3′ and 4′ correspond to $\tilde{n}=7$ and 8, respectively.

pear for $\tilde{n} \geqslant \tilde{n}_{crit} \approx 7$. In dimensional units and for $T \approx 4\,^\circ$K, we find that $n_{crit} \approx 2\times 10^{21}$ cm^{-3} and $k_{crit}^{-1} \approx 1.6 \times 10^{-7}$ cm. For these values of the critical parameters, we have

$$\gamma \equiv \frac{\psi(0)}{T} \gg 1, \tag{1.15}$$

i.e., according to (1.10), $n(r) \ll n_0$ in the region of localization of the electron, and this may be looked upon as a verification of the empty sphere model.

It is interesting to note that, according to (1.13), the critical density is $n_{crit} \sim T^{2/3}$. If we define n_{crit} as corresponding to the end of the intermediate region on the graph of the electron mobility as a function of gas density[5] and if we use the experimental data on electron mobility in the gas at different temperatures,[14] we obtain the comparative graph shown in Fig. 4.[6] Experiment confirms that $n_{crit} \propto T^{2/3}$.

When a strong magnetic field parallel to the z axis is present, the electron can execute infinite motion only along the z axis. However, in one-dimensional problems, any interaction that can be represented by a potential well for the electron should lead to the appearance of electronic bound states (in three-dimensional problems, this well must have a finite depth). It is precisely for this reason that the interaction given by (1.8), which stimulates the deformation of the gas density around the electron (the deformed gas density acts as an effective potential well for the electron), turns out to be sufficient, when the magnetic field is present, to localize the motion of the electron even along the z axis. The mechanism responsible for this localization differs from that discussed above and does not have a threshold with respect to the gas density, so that localized states of magnetic origin are present even for $n < n_{crit}$. The most characteristics feature of such localized states, known as large-radius ions, is the small deformation of the density of gaseous helium in the electron-localization region, which can be formally represented by the condition $\gamma \ll 1$ (this differs from the case of small-radius ions for which, as noted above, $\gamma \gg 1$). Using the fact that γ is small, so that

$$1-\exp\left(-\frac{\psi}{T}\right) \approx \frac{\psi}{T} - \frac{\psi^2}{2T^2},$$

and assuming that

$$\varphi(r, z) = (2\pi)^{-1/2} r_0^{-1} \exp\left(-\frac{r^2}{4r_0^2}\right) \chi(z), \quad r^2 = x^2+y^2, \quad r_0^2 = \frac{c\hbar}{eH},$$

it is possible to obtain an analytic solution for $\chi(z)$ from an Euler equation such as (1.12) by varying the functional (1.11) averaged over r.[12] The result is

$$\chi(z) = \pm (2R_z)^{-1/2} \operatorname{ch}^{-1} \frac{z-z_0}{R_z}, \tag{1.16}$$

where z_0 is an arbitrary constant and R_z and the energy λ_0 of the localized state are, respectively, given by

$$R_z = \frac{2m_e T}{\pi\hbar^2 n_0}\left(\frac{r_0}{a_0}\right)^2, \quad \lambda_0 = -\frac{\hbar^2}{2m_e R_z^2}.$$

The intrinsic energy of a large-radius ion, which is a pure gain in the free energy of the system associated with localization, is $|\lambda_0|/3$. Let us consider some numerical values that are characteristic for a large-radius ion. Let us suppose that $n_0 = 2\times 10^{21}$ cm^{-3}, $T = 4\,^\circ$K, and $H = 5\times 10^5$ G. We then have

$$r_0 \approx 3\cdot 10^{-7} \text{ cm}, \quad R_z = 8\cdot 10^{-7} \text{ cm}, \quad |\lambda_0| \approx 20\,^\circ\text{K}, \quad \gamma = 0.1. \tag{1.16a}$$

Plots of $\delta F_H(\varkappa)$ as a function of $\varkappa$ for $\tilde{n} = 7.8$ have minima even for $n < n_{crit}$ (see the dashed curves in Fig. 3).

2) Experimental studies of the mobility of ions in solid helium are technically more difficult than in the case of the gas. Nevertheless, the first successful results, obtained by Shal'nikov *et al.*[15] and other workers,[16] show that the experimental problem has been solved.

Lack of experimental information and the absence of a rigorous theory prevent the attainment of an unambiguous description of the structure of ionic formations in solid helium. Thus, considerations analogous to those given for the liquid case lead to the idea of complex cation and anion formations in solid helium. In particular, the radius of an empty bubble produced in solid helium subjected to a pressure of about 25–30 atm and due to the introduction of a free electron turns out to be of the order of $R_- \approx 10$–12 Å[17] and does not vary much as the pressure is increased.[18] Such complexes can, of course, move freely through the helium lattice in the form of well-defined quasiparticles with given momenta. In other words, the character of the mobility of the massive helium ions in solid helium is qualita-

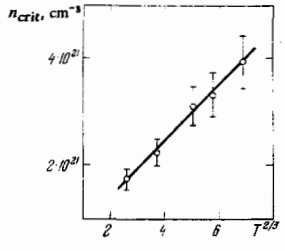

FIG. 4. n_{crit} as a function of temperature according to[14].

[5] The result $n_{crit} \propto T^{2/3}$ was also reported by Khrapak and Yakubov.[13]

[6] The arguments in favor of this definition of n_{crit} are given in Chap. 3, Sec. B.

tively different from that in the liquid situation. However, the relatively small value of R_- as compared with the interatomic distance ($a \approx 3.5$ Å) must be regarded as an indication that this approach to the structure of ions in solid helium is at least arguable.

The alternative possibility is put forward and investigated in detail by Andreev and Meierovich,[19] who look upon ions in solid helium as simple point defects occupying a volume of the order of the volume of one elementary cell of the crystal. The result of this is that the dynamic properties of the ions become identical with the properties of vacancies and uncharged impurities. The theory of the mobility of ions is then essentially based on the quantum-mechanical description of the properties of point defects in solid helium, and turns out to be very fruitful. The great advantage of this approach is the symmetry of the theoretical predictions with respect to positive and negative ions.

2. MOBILITY OF IONS IN THE KINETIC STATE

The mobility of helium ions has a finite value at low temperatures mainly because of single-particle collisions with thermal and impurity excitations of helium. The formal basis for mobility calculations under these conditions is the solution of the corresponding kinetic equation, or some more general approach using the Kubo formalism. Since the main experimental facts can be explained within the framework of kinetic theory, we shall confine our attention in this account to the consequences of this theory.

The classical theory of the mobility of ions in gases, developed by Maxwell, Boltzmann, Langevin, Chapman, Enskog, Kihara, and others contains exhaustive recipes for solving the kinetic equation (in this connection see, for example, Smirnov's review[20]). Nevertheless, modern authors have repeatedly returned to the problem of mobility, and have simplified its solution and redefined its limits of validity. In this connection, it will be useful to write down, without proof, the general expression for the mobility μ of a heavy particle of mass M in a gas of thermal excitations of mass m with a dispersion law $\varepsilon(p)$, energy distribution $n(\varepsilon)$, and momentum $p = mv$. For example, following[21], we have

$$\frac{e}{\mu} = -\frac{m^2}{3}\left(\frac{m}{2\pi\hbar}\right)^3 \int \frac{\partial n}{\partial \varepsilon}\sigma_{tr}(v)\, v^3\, d\mathbf{v}, \qquad (2.1)$$
$$\sigma_{tr} = \int \sigma(v, \theta)(1 - \cos\theta)\, d\Omega$$

where the latter quantity is the transport scattering cross section.

It is shown in[21] that the formula given by (2.1) is valid not only when

$$\sqrt{\frac{m}{M}} \ll 1, \qquad (2.2)$$

but also in more complicated cases (for example, in degenerate He^3–He^4 solutions) when the small parameter of the theory is the quantity

$$\sqrt{\frac{m\varepsilon_F}{MT}} \ll 1, \qquad (2.2a)$$

in which ε_F is the Fermi energy and T the temperature.

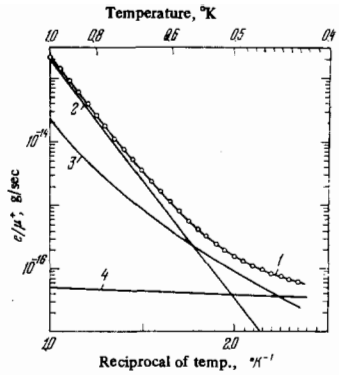

FIG. 5. Temperature dependence of the reciprocal of cation mobility in pure He^4.[24] 1—Experimental points, 2—roton contribution, 3—phonon contribution, 4—proposed contribution of residual impurities.

The equivalent and, evidently, the simplest definition of mobility in terms of wave numbers, which is convenient for calculating the phonon mobility of ions, is given by Baym *et al.*[22]:

$$\frac{e}{\mu} = -\frac{\hbar^2}{6\pi^2}\int dq q^4 \frac{\partial n}{\partial q}\sigma_{tr}(q). \qquad (2.3)$$

The problem for the theory is thus essentially reduced to the determination of the transport cross section for the scattering of an excitation of a particular kind by helium ions, and the subsequent integration of either (2.1) or (2.3).

A. Phonon mobility

1) *Cations.* The phonon mobility of positive ions for $T \lesssim 0.5$ °K is largely determined by collisions between the cations and long-wave phonons. In fact, the cation radius is $R_+ \approx 6$ Å and the wavelength λ_{ph} of thermal phonons for $T \lesssim 0.5$ °K and velocity of sound in He^4 $c_0 = 237$ m/sec is $\lambda_{ph} \approx 3 \times 10^{-7}$ cm, i.e., $R_+ \ll \lambda_{ph}$. The cross section for the scattering of long-wave phonons by a cation under these conditions is of the form $\sigma_{tp} \propto q^4$ (Rayleigh scattering; see[23], p. 366). It is given by

$$\sigma_{tr}(q) = \frac{11 + 2\delta^2 - 4\delta}{9(1+\delta)^2} R_+^6 q^4, \quad \delta = \frac{\rho_l}{\rho_s}, \qquad (2.4)$$

where ρ_l and ρ_s are the densities of the liquid and solid phases, respectively.

The phonon mobility μ_{ph}^+ of cations, given by (2.3) and (2.4), turns out to be proportional to T^{-8}:

$$\frac{e}{\mu_{ph}^+} = \frac{2 \cdot 8!\,\zeta(8)}{27\pi}\frac{(11 - 4\delta + 2\delta^2)}{(2+\delta)^2}\hbar\left(\frac{T}{\hbar c_0}\right)^8 R_+^6, \qquad (2.5)$$

where $\zeta(x)$ is the Riemann zeta function. Four of the powers of temperature in μ_{ph}^+ are due to the scattering cross section, three are due to the number of phonons in liquid helium at low temperatures, and one represents the transfer of momentum from phonons to the ion.

The clearest experimental information on the phonon mobility of cations was obtained by Schwarz and Stark.[24] It is important to note that observation of the phonon mobility of cations in the pure form is a relatively difficult experimental problem. At high temperatures, this mobility is replaced by roton mobility whereas, at low temperatures, the effect of residual impurities becomes appreciable. Measurements of μ^+ and of the proposed contributions to the function $\mu^+(T)$ due to rotons, phonons, and impurity excitations are shown in Fig. 5. Quanti-

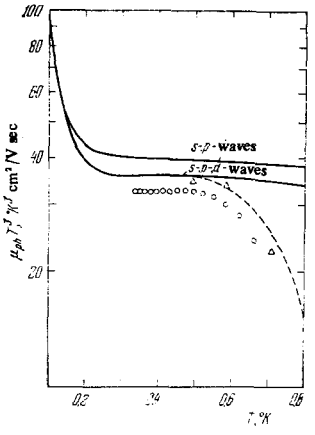

FIG. 6. Temperature dependence of anion mobility in pure He^4. Solid lines—theory,[22] circles—experiment,[26] triangles—[30c].

tative analysis of the data shown in Fig. 5 leads to the conclusion that

$$\mu_{ph}^{+} \propto T^{-\alpha}, \quad \alpha = 7.5 \pm 1, \quad R_{+} \approx 5\text{Å}, \tag{2.6}$$

i.e., the temperature dependence of μ_{ph}^{+} is close to the calculated result, but the numerical value of R_{+} is less than the value predicted by the Atkins model. This discrepancy is fully admissible because the proportionality constant in the expression for $\sigma_{tr}(q)$ given by (2.4) is very arbitrary. For example, by abandoning the solid sphere model, and by taking into account only the existence of the higher-density zero around the nucleating charge, it is possible to show that the cross section for long-wave phonons on the cations is

$$\sigma(\omega) = 4\pi\Lambda^2\omega^4, \quad \Lambda = \int_0^\infty [c_0^{-2} - c^{-2}(r)]\, r^2\, dr,$$

where c_0 and $c(r)$ are the undisturbed and local velocities of sound (the latter is a function of position near the center of the cation).

No attempts have been reported so far to use the numerical value of the constant in (2.6) to interpret the structure of a cation at short distances.

2) *Anions.* At first sight, the phonon mobility of anions at temperatures $T < 1°$ (i.e., where $\lambda_{ph} > R_{-}$) should have a temperature dependence of the form $\mu_{ph}^{-} \propto T^{-8}$, i.e., it should be analogous to the case of the cation and all we should need to consider is the change in the numerical constant in (2.4) and the inclusion of the anion radius $R_{-} \approx 18$ Å. The experiments of Schwarz and Stark[26] have rejected this apparently natural assumption. These measurements (Fig. 6) show that the function $\mu_{ph}^{-}(T)$ is highly nonmonotonic in the region $T = 0.3$–0.5 °K, in which the product $\mu_{ph}^{-} T^3$ is independent of temperature. The formula $\mu_{ph}^{-} \sim T^{-8}$ tends to be followed only when the temperature is reduced to $T < 0.2$ °K.

A qualitative explanation of this feature in the temperature dependence of μ_{ph}^{-}, which is free from adjustable parameters, is given by Baym *et al.*[22] It turns out that the theory of phonon mobility of anions must take into account the natural oscillations of the bubble surface and the possibility of resonance scattering of thermal phonons by these oscillations. To be fair, it is important to note that the spectrum of natural oscillations of the anion surface was calculated previously by other workers.[27] However, it was only Baym *et al.*[22] who pointed out that the fundamental frequency of the natural-anion oscillations was of the same order as the frequency of the thermal phonons at $T \sim 0.4$ °K and, consequently, such phonons should undergo resonance scattering by the anion.

The spectrum of the surface oscillations of a charged bubble arises from the balance equation for all the pressures acting on the surface of the deformed bubble, just as in the classical problem of the oscillations of an incompressible drop. The only quantity that requires special definition is the electron pressure on the anion surface

$$P_i^{el} = \Pi_{ik} n_k,$$
$$\Pi_{ik} = \frac{\hbar^2}{4m_e}\left(\frac{\partial\psi}{\partial x_i}\frac{\partial\psi^*}{\partial x_k} - \psi\frac{\partial^2\psi^*}{\partial x_i \partial x_k} + \text{c.c.}\right). \tag{2.7}$$

In these expressions, Π_{ik} is the momentum flux tensor for an electron localized inside the bubble and n_k is the normal to the anion surface. It is assumed that the electron wave function ψ in the bubble can follow adiabatically any small deformation of the surface.

Let us now collect together all the additions to the pressure on the oscillating surface. They are: the electron component, the addition due to surface tension, and the hydrodynamic part of the pressure which represents the time-dependent character of the problem. Since the sum of all the pressures must be equal to zero, the spectrum of the oscillations of the anion surface is given by

$$\omega_0^2 = \frac{8\sigma}{\rho R_{-}^3},$$
$$\omega_l^2 = \frac{\sigma}{\rho R_{-}^3}(l+1)(4\pi S_l + l^2 + l + 2), \quad S_l = \frac{j_l'}{j_l} - \frac{j_0''}{2j_0'}\Big|_{x=\pi}, \quad l \geqslant 2. \tag{2.8}$$

In these expressions, σ is the surface tension, ρ is the density of helium, and $j_l(x)$ are the spherical Bessel functions. The fundamental frequency ω_0 corresponding to the radial oscillations of the bubble for $\sigma \approx 0.36$ erg/cm^2 and $R_{-} = 18$ Å is of the order of $\omega_0 \approx 10^{10}$–10^{11} sec^{-1}, i.e., it is, in fact, in the region of the phonon frequencies corresponding to ~ 0.3–0.5 °K. The cross section for the scattering of such phonons in the presence of a single resonance frequency ω_0 has the following well-known form[28]:

$$\sigma(\omega) = \frac{4\pi R_{-}^2}{[(\omega_0^2/\omega^2) - 1]^2 + q^2 R_{-}^2}, \tag{2.9}$$

where q is the phonon wave number and $qR_{-} \ll 1$.

In the more general case of several natural frequencies, the cross section exhibits resonance peaks corresponding to further resonances. Figure 7 shows the overall appearance of the function $\sigma(q)$ for an anion. This curve was calculated in[22]. The corresponding anion mobility that follows from (2.3) when the numerical values of $\sigma(q)$ are inserted (see Fig. 7) is shown in Fig. 6 together with the experimental points. In view of the

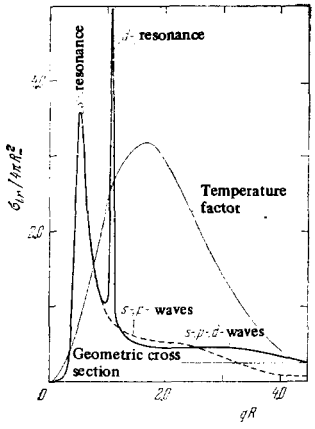

FIG. 7. Transport cross section for the scattering of phonons by anions.[22] Two variants are shown: cross section corresponding to the scattering of s and p waves and cross section corresponding to the scattering of s, p, and d waves. In addition, the graph shows the temperature factor $q^4\partial n(q)/\partial q$ for $T = 0.5$ °K, in arbitrary units.

fact that the theory does not contain adjustable parameters, it must be admitted that the agreement between the theoretical and experimental values of $\mu_{ph}^-(T)$ is very good.

To complete the picture, it will be useful to summarize the results obtained from studies of the effect of an external pressure on the phonon mobility of anions, obtained by Ostermeier.[29a] An external pressure will reduce the radius of the bubble and, consequently, increase the frequencies of its natural oscillations. The result of this is that the region corresponding to the resonance phonon-anion scattering is shifted toward higher temperatures. Figure 8 illustrates the variation that occurs in the resonance phonon-anion scattering cross section where an external pressure is applied. The dependence of the anion radius on external pressure, which follows from experimental data on the phonon mobility of anions, is shown in Fig. 9. This figure also gives the results of other experiments on the pressure dependence of R_- together with the results of theoretical calculations.[10] The agreement between the various experimental curves among themselves and with the calculated values of $R_-(P)$ may be regarded as good.

B. Mobility of ions in weak solutions

The mobility of a massive solid sphere in a Boltzmann gas of impurity excitations should be of the form $\mu_3 \propto T^{-1/2}$.[7)] This prediction is valid for helium ions within the framework of the Atkins model and is, in general, in conflict with observations. In the case of cations, the impurity mobility μ_3^+ is independent of T in a broad range of temperatures. This is clearly illustrated by graphs of the temperature dependence of this mobility, shown in Figs. 10 and 11 (they are taken from the work of Essel'son, Kovdrya, and Shikin[30a] and Kuchnir, Ketterson, and Roach[31]). For anions, the impurity mobility μ_3^- is a nonmonotonic function of temperature (see Fig. 12, which shows the data from[31]). Thus, just as in the case of μ_{ph}^+, we are forced to consider separately the temperature dependence of the two mobilities μ_3^+ and μ_3^-.

1) *Cations.* The main reason for the failure of the solid sphere model of the interaction between cations and low-energy impurity excitations in the presence of the excess pressure around the positive ion which decreases in inverse proportion to a certain power of the distance. The parametrization of the resulting scattering problem is such that the main contribution to the cross section for the scattering of thermal impurity excitations by a cation is due to the excess-pressure "tail" at distances appreciably greater than the Atkins radius.

To obtain a qualitative description of the interaction between cations and impurity excitations, we note that He^4 and He^3 atoms located in the neighborhood of a bare charge experience two forces, namely, polarization attraction toward the center of the cation and repulsion due to the excess pressure near the cation. These forces cancel out in the case of He^4 atoms, so that a stationary region of enhanced solvent pressure appears in the neighborhood of the original charge. In the case of He^3, on the other hand, which has the same polarizability as He^4 but a somewhat greater effective volume ($v_3/v_4 \approx 1.27$[32]), the repulsive forces exceeds the attractive force. The difference between these two forces, and together with them the interaction between the cation and impurity excitation, $V_3^+(r)$, turn out to be different from zero. When the definition of pressure given by (1.1) in the neighborhood of the cation is taken into account, the interaction $V_3^+(r)$, which is, in fact, a repulsion, takes the form

$$V_3^+(r) = \frac{\beta^2}{r^4}, \quad \beta^2 = \frac{1}{2}\alpha e^2\left(\frac{v_3}{v_4} - 1\right). \tag{2.10}$$

The macroscopic character of the definition of the energy V_3^+ (for example, we have used the concept of pressure in a fluid, and so on) means that the energy of the incident impurity excitations must be confined to values below a certain figure. A suitable criterion for this is

$$r_{\min} > R_+,$$

where R_+ is the Atkins radius and $r_{\min}$ is the minimum separation between the impurity excitation and the cation center in a head-on collision, so that

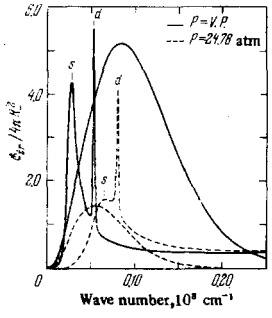

FIG. 8. Transport cross section for the scattering of phonons by anions in pure He^4 at different external pressures.[29a] Solid line—zero pressure; broken line—24.78 atm.

[7)] This temperature dependence of μ_3 has a simple explanation, just as in the case of μ_{ph}^+. In this situation, the impurity concentration and the cross section for the scattering of impurity excitations by the sphere are independent of temperature. The only quantity which does depend on temperature is the transferred momentum: $p_T \propto \sqrt{T}$. Hence, it follows that $\mu_3 \propto T^{-1/2}$.

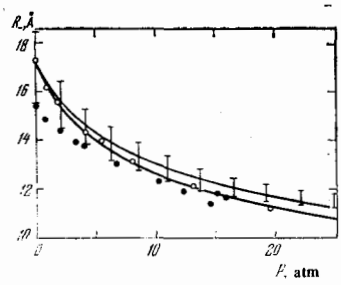

FIG. 9. Anion radius as a function of external pressure. Solid lines—theoretical[10]; open circles—Springett[29b]; full points—Zipfel and Sanders[29c]; bars—Ostermeier.[29a]

$$V_3^+(r_{\min}) \sim T, \quad r_{\min}^4 \approx \frac{\beta^2}{T}. \tag{2.11}$$

For temperatures $T \sim 1$ °K, the separation $r_{\min}$ that follows from this equation is $r_{\min} \gtrsim 9\times10^{-8}$ cm, i.e., the inequality $r_{\min} > R_*$ is, in fact, satisfied. Consequently, the problem of scattering of impurity excitations by cations at $1 \lesssim 1$ °K can be solved as a problem involving scattering by a power-type potential without taking into account the structure of the cation nucleus. This was first noted by Essel'son *et al.*[30a] and, independently, by Bowley and Lekner.[33]

The nonrelativistic quantum theory of scattering by a potential of the form $V(r) \sim r^{-4}$ has been developed to a reasonably complete state in connection with the classical problem of the mobility of electrons in a gas of neutral atoms in which the interaction is, in fact, an attraction. The main point of the theory is that the wave equation for an electron in a potential $V \sim r^{-4}$ can be reduced to a Mathieu equation with an imaginary argument and, thereafter, the scattering amplitude is determined in terms of known special functions.[34] This is also possible for the respulsive potential $V_3^+ = \beta^2 r^{-4}$. Moreover, this problem is free from the difficulties encountered in the case of attraction because there is now no danger that the particle will fall into the attractive center.

The overall result is that the asymptotic behavior of the transport cross section for the scattering of impurity excitations by a cation is as follows:

$$\sigma_{tr}(q) = \begin{cases} \frac{8\pi}{3} f_0 q^{-1}, & qf_0 \gg 1, \\ 4\pi f_0^2 \left(1 - \frac{16}{15}\pi q f_0\right), & qf_0 \ll 1, \end{cases} \qquad f_0^* = 2m_3\beta^2\hbar^{-2}; \tag{2.12}$$

where q and m_3 are, respectively, the wave number and mass of the impurity excitation and f_0 is the zeroth scattering amplitude. The numerical value of the quantum length f_0 for a cation in helium is of the order of $f_0 \approx 6\times10^{-7}$ cm. Consequently, the quantum limit of scattering begins to be realized only in the region of very low temperatures. For all other temperatures $(2m_3T)^{1/2}\hbar^{-1} \gg f_0^{-1}$, the scattering process is quasiclassical. Moreover, $\sigma_{tr} \propto q^{-1}$, which is qualitatively different from a collision between solid spheres and is sufficient to explain the fact that the mobility μ_3^+ is independent of T in a broad range of temperatures.

Substituting the quasiclassical behavior of $\sigma_{tr}(q)$, given by (2.12), into (2.1), we obtain[30a,35]

$$\mu_3^+ = \frac{r}{5.32 n_3 \beta \sqrt{m_3}}, \tag{2.13}$$

where n_3 is the concentration of the impurity atoms in the solution and β is given by (2.10). The mobility giv-

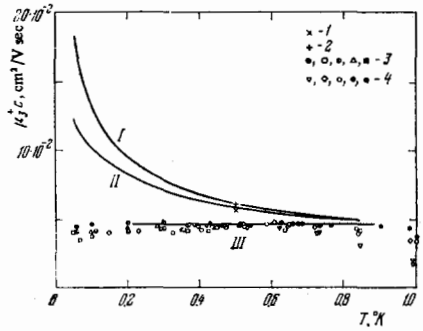

FIG. 10. Impurity mobility of cations as a function of temperature.[30a] Solid lines: I—Atkins model with cross section $\sigma_{tr} = \pi R^2$ ($R = 7$ Å); II—same model but corrected for the quantum increase in the scattering cross section from πR^2 to $4\pi R^2$; III—mobility determined from (2.13). Experimental points: 1) 1.3×10^{-3}%; 2) 5.1×10^{-3}%[30c]; 3) from 1.55×10^{-20}% to 4.46%[30b]; 4) from 0.75% to 39.9%.[30a]

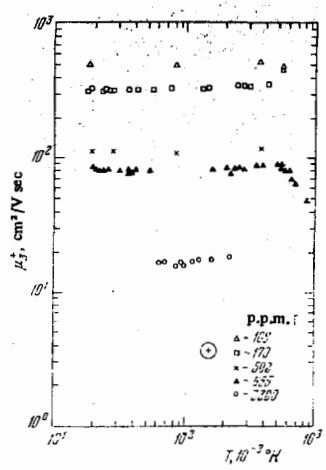

FIG. 11. Mobility μ_3^+ as a function of temperature T, according to[31].

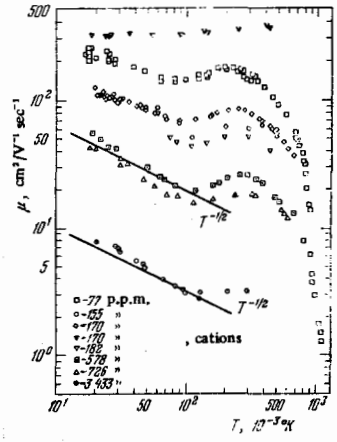

FIG. 12. Mobility μ_3^- as a function of temperature T, according to[31].

en by (2.13) is independent of temperature. This result was known to Maxwell[35] in the case of the mutual diffusion of two gases with a repulsive interaction of the form $V(r) \propto r^{-4}$. When the particular value of β is taken into account, the mobility given by (2.13) gives a good description of the experimental data not only in the sense that it predicts the correct temperature dependence but also because it yields the correct absolute value without the use of adjustable parameters. Figure 10 shows a comparison between the calculated and experimental values of the impurity mobility μ_3^+ taken from[30a]. A similar comparison, which confirms the validity of the above interpretation of the interaction between low-energy impurity excitations and cations, is given in[33].

2) *Anions.* The most likely reason for the observed anomalies in the temperature dependence of the mobility of anions in weak He^3–He^4 solutions is the adsorption of impurity excitations on the anion surface. The corresponding phenomenon on the plane surface of a weak solution is well known[36] and gives rise to a characteristic temperature dependence of the surface tension of weak solutions. It is natural to suppose that the anion surface can also adsorb impurity excitations.

Let us adopt the adsorption interpretation of the temperature dependence of μ_3^- and consider the most complete data that are available on this temperature dependence. They are given in[31] and are illustrated in Fig. 12. It follows from these data that, at very low temperatures, the anion mobility is $\mu_3^- \propto T^{-1/2}$. If the impurity excitations have a Boltzmann velocity distribution, this type of dependence of μ_3^- on T is, as already noted, characteristic for the motion of a solid sphere in a gas of impurities[8)]:

$$\mu_3^- = \frac{3e}{8\pi_3 \tilde{R}_-^2 \sqrt{2\pi m_3 T}}. \qquad (2.14)$$

$\tilde{R}_-$ is the effective radius of the solid sphere. Numerical values of $\tilde{R}_-$ that follow from the experimental data[31] at low temperatures, and the values of μ_3^- given by (2.14), are collected in Table I and turn out to be $\tilde{R}_- \approx 27 \pm 1$ Å, i.e., they exceed appreciably the characteristic value of R_- for an anion in pure He^4.

As the temperature increases, the cross section for the scattering of volume impurity excitations is found to decrease sharply in a relatively narrow temperature interval, giving rise to an increase in the anion mobility in this temperature band. Thereafter, the anion size ceases to vary, assuming the value $R_-^0 \approx 20$ Å, which is not very different from the R_- in pure He^4. It is natural to associate this change in the cross section for the scattering of impurity excitations by anions with the "escape" of impurities adsorbed on the anion surface into the body of the liquid helium. As the impurity surface levels are emptied with increasing temperature, the effective anion size ceases to depend on temperature.

TABLE I. Anion parameters in weak He^3–He^4 solutions, obtained from experimental data.[40]

c	$c\mu_3^-$, arbitrary units ($T = 0.05$ °K)	$\tilde{R}_-$, Å	R_-^0, Å	T_F^*, °K	ε_L, °K
$3.43 \cdot 10^{-3}$	$5 \cdot 3.42 = 17.3$	26		0.15±0.02	0.27±0.03
0.726	$24 \cdot 0.726 = 17.4$	27	19	0.10	0.28±0.04
0.578	$30 \cdot 0.578 = 17.3$	27	18	0.09	0.26±0.04
0.170	$90 \cdot 0.170 = 15.3$	28.9	19	0.07	0.26±0.05
0.077	$180 \cdot 0.077 = 14$	31	20	0.06	0.26±0.06

It is clear from the table that the product $c\mu_3^-$ begins to depend on c in the region of low concentrations. For this reason, the values of $\tilde{R}_-$ and R_-^0 obtained for the last concentration $c = 0.077 \times 10^{-3}$ are too high and were not included in the calculation.

Unfortunately, the influence of impurities adsorbed on an anion surface on its mobility in weak He^3–He^4 solutions is not equivalent to a change in the surface tension which would define the radius of the anion. In addition to this channel, which is sensitive to the presence of surface impurities, and can be used to obtain a rigorous description in terms of a phenomenological law of dispersion for the surface impurities throughout the temperature range, there is a direct interaction between the surface and volume impurity excitations. The absence of a clear theory of this interaction which provides an appreciable contribution to the anomalous behavior of the temperature dependence of μ_3^- impedes the development of a rigorous theory of mobility of anions in weak solutions of helium. At present, there are only certain qualitative ideas that can be used to estimate the parameters of the spectrum of impurity excitations on the anion surface.

The formal problem of the properties of s impurities on a spherical surface begins with the determination of the excitation spectrum. As in the case of the plane surface, this problem has a simple solution for a low-lying energy level[37]:

$$\varepsilon_l = -\varepsilon_0 + \chi l(l+1), \qquad (2.15)$$
$$\chi = \frac{\hbar^2}{2m_s \tilde{R}_-^2}, \quad \chi l(l+1) < \varepsilon_0, \quad l = 0, 1, 2, \ldots;$$

where $\varepsilon_0 > 0$, m_s is the mass of the s impurity, and the energy ε_l is measured from the bottom of the v-impurity band. The expression given by (2.15) is valid when $\tilde{R}_- \gg \lambda$, where λ is the characteristic length for the attenuation of wave functions of s impurities within the liquid. In our case, when $\tilde{R}_- \gg 20$ Å and $\lambda \sim \hbar(2m_s\varepsilon_0)^{-1/2}$ ($\varepsilon_0 \approx 2$ °K, $m_s \approx 10^{-23}$ g, i.e., $\lambda \approx 2$–3 Å), the condition $\tilde{R}_- \gg \lambda$ is, in fact, satisfied. It is important to note that, in general, the spectrum of s impurities on a sphere and the spectrum on a plane surface have a more complicated form: $\varepsilon_{nl} = -\varepsilon_n^0 + \chi l(l+1)$. This is illustrated by the model example considered in[37]. For particular values of ε_0 and m_s, known from the two-dimensional problem, the probability of the existence of levels with $n > 0$ turns out to be less than or of the order of one-half.

Once we have the excitation spectrum, we can readily

[8)] To obtain (2.14), we substitute the short-wave limit of the scattering amplitude f of impurity excitation on a sphere of radius $\tilde{R}_-$ in (2.1). In this limit, $f(\theta) = (\tilde{R}_-/2) + f_1(\theta)$ (see[28], p. 451), where $f_1(\theta)$ is the so-called "shadow" peak in the scattering amplitude which is nonzero at small angles θ. The contribution of this peak to the transport cross section turns out to be equal to zero. As a result, $\sigma_{tr} = \pi\tilde{R}_-^2$ and (2.1) assumes the form given by (2.14).

establish the relation between the total number N_s of s impurities and the chemical potential of the given system:

$$N_s = \sum_{l=0}^{L} 2(2l+1)\left[\exp\left(\frac{\varepsilon_l - \mu_s}{T}\right) + 1\right]^{-1}; \qquad (2.16)$$

where ε_l is given by (2.15) and $L = l_{max}$ is defined by the requirement that

$$\varepsilon_0 - \chi L(L+1) \geqslant 0. \qquad (2.16a)$$

It follows from general thermodynamic considerations[38] that the magnitude of the chemical potential μ_s must be equal to the chemical potential μ_v of the impurities filling the volume of the solvent:

$$\mu_s = \mu_v, \quad \mu_v = -T \ln\left[\frac{2m_4}{c\rho}\left(\frac{m_3 T}{2\pi\hbar^2}\right)^{3/2}\right], \qquad (2.17)$$

where ρ is the solvent density, c is the relative volume concentration of the solution, and m_3 and m_4 are the He^3 and He^4 masses under volume conditions.

Combining (2.16) and (2.17), we have

$$N_s = \sum_{l=0}^{L} 2(2l+1)\left[\frac{2m_4}{c\rho}\left(\frac{m_3 T}{2\pi\hbar^2}\right)^{3/2}\exp\left(-\frac{|\varepsilon_l|}{T}\right) + 1\right]^{-1}. \qquad (2.18)$$

This relates N_s and c, i.e., it solves the above problem of the dependence of N_s on the volume parameters of the solution.

As already noted, the mobility of ions at low temperatures is sufficiently well represented by (2.14) with $\tilde{R}_- \approx 27 \pm 1$ Å. As the temperature rises, the s impurities begin to leave the s levels. The onset of this process corresponds to the neighborhood of the minima on the curves in Fig. 12. The position of the minima on the $\mu_3^-(T)$ curve will thus qualitatively characterize the degeneracy temperature T_F^s for s impurities on the surface levels. Using (2.18) for N_s, we can readily determine T_F^s from

$$\frac{2m_4}{c\rho}\left(\frac{m_3 T_F^s}{2\pi\hbar^2}\right)^{3/2}\exp\left(-\frac{|\varepsilon_L|}{T_F^s}\right) \approx 1. \qquad (2.19)$$

Using this expression and the experimental values of c and T_F^s, which determine the positions of the minima on $\mu_3^-(c, T)$, we can estimate the shallowest surface level ε_L. The values of ε_L, calculated for different concentrations c, are collected together in the above table. The fact that ε_L remains roughly constant as c varies in a broad range of values indicates that T_F^s has been reasonably chosen.

The observed increase ΔR in the anion radius for $T \ll T_F^s$ is the same for different concentrations of the solution (see table) and, together with the temperature-independent limit for N_s

$$N_s|_{T\to 0} \to \sum_{0}^{L} 2(2l+1),$$

the existence of which qualitatively justifies the appearance of ΔR, can be regarded as clear evidence for the existence of s impurities on the anion surface. Moreover, the observed values of ΔR and ε_L, together with qualitative discussions[37] of the reasons for the increase in R (due to the change in the surface tension and the direct interaction between the v and s impurities) enable us to estimate the parameters of the spectrum of impurity excitations: $\varepsilon_0 \lesssim 2.4$–$2.5$ °K, $m_s \lesssim 1.2 \times 10^{-23}$ g, and $L \sim 17$–18.

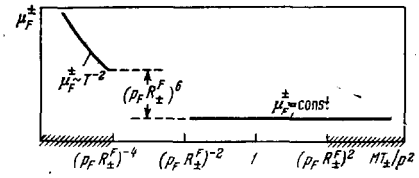

FIG. 13. Position of temperature intervals in which the mobility of charges in liquid He^3 can be calculated from the kinetic equation.[39] The corresponding temperature intervals are shaded. The values of $\mu_F^{\pm}(T)$ in these intervals are indicated.

C. Fermi-particle mobility

If we consider the various mechanism responsible for the low-temperature mobility of helium ions in order of increased complexity, we must introduce the Fermi particle mobility after the phonon and impurity mobilities. The Fermi particle mobility is observed when

$$T \ll \varepsilon_F, \qquad (2.20)$$

where ε_F is the Fermi energy of pure He^3 or of He^3 in the He^3–He^4 solution.

The first serious problem for the theory of Fermi-particle mobility of ions arises in connection with the desire to have the usual kinetic equation for particular calculations. Analysis of this question, performed in the most complete form by Mel'nikov,[39] shows that, for charged particles of radius R with $\xi = p_F R \gg 1$, where p_F is the Fermi momentum, the kinetic equation exists both at high and low pressures. The results reported in[39] are illustrated schematically in Fig. 13. The regions of existence of the kinetic equations are shaded. For low temperatures, $T \lesssim \xi^{-4}$ and $\mu_F^{\pm} \propto T^{-2}$. At intermediate temperatures, for which the kinetic equation is not valid, the mobility is reduced by a factor of ξ^6.

The existence of a high-temperature asymptotic behavior of $\mu_F^{\pm}$, which is independent of temperature, was first established by Davis and Dagonnier.[21] By analyzing the range of applicability of the Fokker–Planck method of transforming the collision integral to a differential form, the authors of[21] showed that, when $T \ll \varepsilon_F$, this could be done provided

$$\frac{m_3}{M_\pm} \ll \frac{T}{\varepsilon_F} \ll 1,$$

where m_3 is the effective mass of the impurity. Under these conditions, the mobility is given by (2.1) or, in explicit form,

$$\mu_F^{\pm} = \frac{3\pi^2 e\hbar^3}{2m_s^3 \sigma_{tr}^{\pm}(q_F)\varepsilon_F^3}, \qquad (2.21)$$

where $\sigma^{\pm}_{tr}(q_F)$ is the transport cross section for the scattering of Fermi particles by a helium ion. As the temperature is reduced until $T < \xi^2$, the arguments used in[21] lose their force. However, a more general analysis, given in[39], leads to the conclusion that (2.21) will remain valid down to temperatures $T \gtrsim \xi^{-2}$ (see Fig. 13). Violation of the inequality $T \ll \varepsilon_F$ in the direction of increasing temperature leads to the appearance of Fermi-liquid corrections to the temperature dependence of ion mobility. The most important of these is proportional to $T^2 \ln T$.[40]

At low temperatures, $T \ll (m_3/M_\pm)\varepsilon_F$, the restriction on the region of integration with respect to the momentum of the ion in the collision integral of the kinetic equation, which enables us to use the Fokker–Planck approximation, becomes unimportant because scattering then occurs only through small angles. Denoting by $f_0^\pm$ the zero-angle scattering amplitude, linearizing the original kinetic equation with respect to the electric field E, and using dimensionless variables, we obtain the following expression for the mobility at low temperatures[39]:

$$\mu_F^\pm = \frac{2\pi^{1/2}e\hbar^3}{2M_\pm^2 T^2 (f_0^\pm)^2} \int_0^\infty \varphi(x)\, e^{-x^2} x^3\, dx, \qquad (2.22)$$

where the function $\varphi(x)$ is determined by the following equation:

$$-xe^{-x^2} = \left\{ \int_0^x \frac{y^2}{x^2} \left[\frac{y\varphi(y)}{3} - x\varphi(x) \right] + \int_x^\infty \left[\frac{x\varphi(y)}{3} - y\varphi(x) \right] \right\} \frac{x^2 - y^2}{e^{x^2} - e^{y^2}}\, dy.$$

Several authors[41] have obtained $\mu_F^\pm \propto T^{-2}$ at low temperatures. It is also interesting to note that the mobility given by (2.22) is inversely proportional to the square of the ion mass, i.e., $M_\pm^{-2}$. The appearance of M in the expression for μ_F is characteristic for situations in which the momentum of incident excitations substantially exceeds the thermal momentum of the ion.

For strong degeneracy, $T \ll \varepsilon_F$, and the dependence of the transport cross section on the wave number of the incident excitations does not influence the temperature behavior of the mobility. This is why the explicit form of the function $\sigma^\pm_{tr}(q_F)$ is not usually discussed in the theory of Fermi particle mobility (in contrast to the case of phonon and impurity mobilities). At the same time, this question is significant when we investigate the behavior of $\mu_F^\pm$ as a function of the Fermi energy of the incident Fermi particles. This can be done experimentally by introducing charged particles into degenerate He^3–He^4 solutions and varying the He^3 concentration. The expected effect can be predicted, at least for positive ions. By taking into account the definition of the transport scattering cross section for impurity excitations on a cation, given by (2.12), and the range of validity of these definitions, we can readily find the function $\mu_F^+(\varepsilon_F)$ for a cation in weak degenerate He^3–He^4 solutions[42]:

$$\mu_F^+ = \frac{3\pi^2 e\hbar^3}{2m_3^3\varepsilon_F} \times \begin{cases} \dfrac{1 + (16/15)\,\pi f_0 q_F}{4\pi f_0^2}, & q_F f_0 \ll 1, \\ \dfrac{3}{8\pi} q_F f_0^{-1}, & R_+^{-1} \gg q_F \gg f_0^{-1}, \end{cases} \qquad (2.23)$$
$$f_0^2 = 2m_3\beta^2\hbar^{-2};$$

where β^2 is given by (2.10) and R_+ is the Atkins radius.

Let us now compare the theoretical predictions with observations.

1) The presence of a temperature-independent asymptotic behavior of $\mu_F^\pm$, predicted by (2.21), can be compared with the experimental data of Anderson *et al.*[43] (see Figs. 14 and 15), which confirm the existence of this plateau. Comparison of the experimental and calculated values of μ_F^- (2.21), using $\sigma^-_{tr} = \pi (R_-^F)^2$ (R_-^F is the geometric radius of the anion in pure He^3), enables us to estimate R_-^F. This yields $R_-^F \approx 20$ Å, which is in reasonable agreement with the numerical value of R_-^F (1.5) for liquid He^3.

The value of R_+^F deduced from experimental data on μ_F^+ and μ_F^- in the neighborhood of the plateau, and from the expression for the mobility μ_F^+ given by (2.21), can conveniently be written in the form

$$\frac{R_F^+}{R_F^-} \approx \sqrt{\frac{1}{5}}. \qquad (2.24)$$

Since $R_-^F \approx 20$ Å, we have the estimate $R_+^F \approx 9$–10 Å. This result for R_+^F exceeds somewhat the Atkins radius $R_+ \approx 6$–7 Å. The structure of R_+^F remains an open question.

2) At low temperatures, the ion mobility should in-

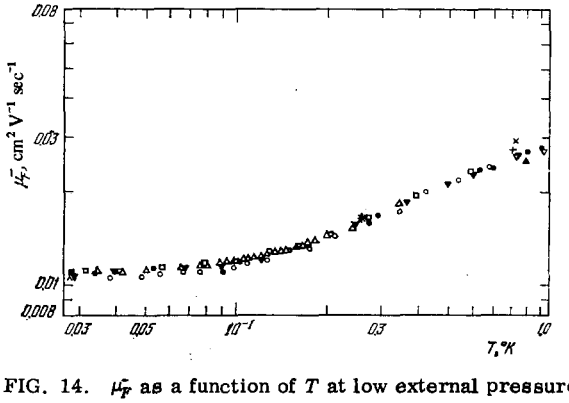

FIG. 14. μ_F^- as a function of T at low external pressure.[43] The various series of points shown in Figs. 14 and 15 correspond to cells of different design at pressures in the range 0–78 cm Hg.

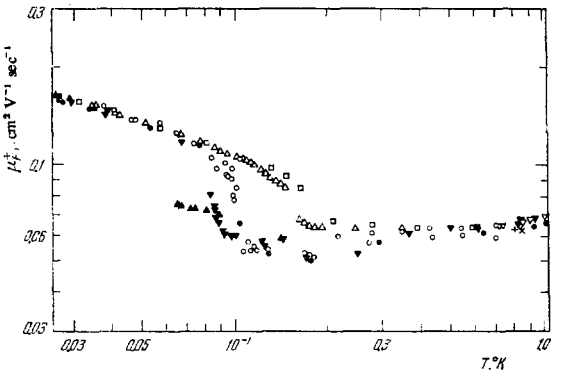

FIG. 15. μ_F^+ as a function of T at low external pressures.[43]

crease with temperature, in accordance with $\mu_F^{\pm} \sim T^{-2}$. A tendency to increase mobility should, according to[39] (see Fig. 13), appear earlier for ions with the smaller radius, i.e., the cations. This is, in fact, confirmed by experiment. It is clear from Figs. 14 and 15 that the mobility μ_F^+ begins to increase toward lower temperatures at higher T than the mobility μ_F^-. However, the asymptotic behavior $\mu_F^{\pm}|_{T\to 0} \propto T^{-2}$ has not as yet been confirmed experimentally.

3) Attention is called to the increased mobility as the temperature increases from the region $T/\varepsilon_F \ll 1$ to the region $T/\varepsilon_F \lesssim 1$. This behavior is largely hydrodynamic in origin since the inequality $l/R \lesssim 1$ begins to be satisfied in this temperature region (l is the free path of the Fermi excitations), and the viscosity η of the Fermi liquid decreases with increasing temperature as $\eta \sim T^{-2}$.[44] The insufficiently small value of the parameter $l/R \lesssim 1$ during the initial stage of the increase in mobility complicates the temperature dependence which then takes the form $\mu_F^{\pm}|_{T\leqslant\varepsilon_F} \propto T^2 \ln T$.[40]

D. Roton mobility

At temperatures $T \gtrsim 0.8$ °K, the mobility of ions in pure He^4 begins to be limited by collisions with rotons. Under the "kinetic conditions," when $0.8 \leqslant T \leqslant 1.7$ °K, the main contribution to the mobility of ions is due to single-particle collisions with rotons. For temperatures $T \gtrsim 1.8$ °K, on the other hand, the interactions of rotons with one another become appreciable, and the ion mobility assumes the Stokes character.

Several experiments,[45] performed under kinetic conditions, have led to the conclusion that the temperature dependence of roton mobility of ions is essentially exponential in form, but the activation energies $\Delta^{\pm}$ are different:

$$\mu_{rot}^{\pm} \propto \exp\left(-\frac{\Delta^{\pm}}{T}\right), \tag{2.25}$$

where $\Delta^+ = 8.65$–8.8 °K, $\Delta^- = 7.7$–8.1 °K. For comparison, the gap Δ in the roton part of the spectrum of pure He^4 at zero pressure is $\Delta = 8.6$ °K.[44]

Attempts to interpret the observed deviations of the temperature dependence of $\mu_{rot}^{\pm}$ from the law $\mu_{rot}^{\pm} \propto e^{-\Delta/T}$ have encountered a number of serious difficulties.

1) First of all, the momentum p_0 of rotons is high and comparable with the thermal momentum p_T^i of ions at $T \sim 1$ °K. This resembles the Fermi particle situation except that, in the problem of Fermi particle mobility, there are definite temperature intervals (both at high and low temperatures; see Fig. 13) for which the kinetic description of the motion of ions through a Fermi gas turns out to be relatively simple. It is precisely in this region that the calculation of $\mu_F^{\pm}$ could be taken to completion. In the roton problem, on the other hand, the temperature cannot be varied within broad limits. The required solution should refer to the temperature region $0.8 \lesssim T \lesssim 1.7$ °K, where the ratio p_0/p_T^i is of the order of unity. Under these conditions, it is very difficult to investigate the kinetic equation for ions moving through a roton gas. Nevertheless, the kinetic equation has been

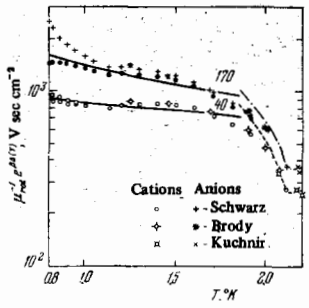

FIG. 16. Temperature dependence of roton mobility $\mu_{rot}^{\pm}$. Solid lines—calculation[47] with the following parameter values: cations—$R_1 = 0$, $R = 9.81$ Å, $M = 40 m_{He^4}$; anions—$R_1 = 0$, $R = 18.65$ Å, $M = 170 m_{He^4}$. Experimental points: Schwarz,[45b] Brody,[45c] Kuchnir.[53b]

used to calculate the roton mobility of ions. The best-founded results in this direction were obtained by Bowley[46] and Barrera and Baym.[47] These workers used the method put forward by Josephson and Lekner[48] for the solution of the problem of Fermi particle mobility, which enabled them to take into account the finite value of the parameter $\zeta_{\pm} = p_0^2(p_T^i)^2 \equiv p_0^2/2TM_{\pm}$ in the course of the solution of the kinetic equation. The final expression for $\mu_{rot}^{\pm}$ obtained from a variational principle is as follows[47]:

$$\frac{e}{\mu_{rot}^{\pm}} = \frac{4\pi^{1/2}}{3}\rho_n v_{rot}[R^2 F(\zeta_{\pm}) + R_1^2 F_1(\zeta_{\pm})], \tag{2.26}$$

$$F(x) = x^{-1} + e^{-x}[xK_0(x) - (1+x)K_1(x)],$$

$$F_1(x) = \frac{1}{10}x^{-2} + \frac{1}{10}e^{-x}\left[\left(3x + \frac{1}{2}\right)K_0(x) - (3x - 1 - x^{-1})K_1(x)\right];$$

where ρ_n is the roton density, v_{rot} is the thermal velocity of rotons, R, R_1 are constants of the theory, and K_0, K_1 are Bessel functions of an imaginary argument. As $\zeta \to 0$, $F(\zeta) \to 0$, we have $F_1(\zeta) \to 3/8$ and the expression given by (2.26) assumes the simpler form:

$$\frac{e}{\mu_{rot}} \to \sqrt{\frac{\pi}{2}} R_1^2 \rho_n v_{rot}. \tag{2.27}$$

This result can be obtained from elementary kinetic considerations. In the opposite limiting case, when $\zeta \gg 1$ (this is possible formally for $p_0 \to \infty$), we have $F(\zeta) \propto \zeta^{-1}$ and $\mu_{rot}^{\pm} \propto (M_{\pm})^{-1}$. In other words, in this limit, the dependence of $\mu_{rot}^{\pm}$ on $M_{\pm}$ is similar to the dependence of $\mu_F^{\pm}$ on $M_{\pm}$, given by (2.22).

Barrera and Baym[47] have shown that the expression for $\mu_{rot}^{\pm}$ given by (2.26) provides a satisfactory description of the observed difference in the behavior of $\mu_{rot}^{\pm}(T)$ when the constants R, R_1, M_+, and M_- are suitably chosen (Fig. 16). The main reason for the difference in $\mu_{rot}^{\pm}(T)$ in this interpretation is the difference between the $\zeta_{\pm}$ for cations and anions. This proposition has stimulated the publication of the interesting experimental paper by Glaberson and Johnson.[49] These workers have found a method of introducing singly ionized atoms of different elements into helium and were able to vary the mass of the helium ions. They were thus able to measure the dependence of μ_{rot} on M. Unfortunately, the results reported in[49] are not in agreement with

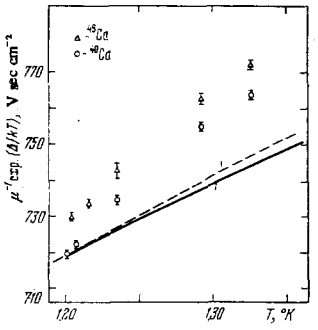

FIG. 17. Roton mobility of ^{48}Ca and ^{40}Ca ions with equal charges but different bare masses.[49] The variation in the ion mass does not lead to the expected[46,47] change in the slope of the temperature dependence of mobility. Solid curve—theoretical line lying nearest to the experimental points obtained from (2.26) with $R_1/R = 0$ and $M = 53m_{He^4}$. Broken curve—analogous maximum possible approach to the experimental points which follow from[46].

(2.26), and the discrepancy is shown in Fig. 17.

2) The other trouble with the theory of roton mobility, which, by the way, has been ignored in[46,47], is connected with adsorption phenomena. In the case of cations, this involves localized roton states in the region of excess pressure[9)] surrounding the bare charge.

For anions, the existence of surface roton states is less obvious but their presence can be admitted by adopting the hypothesis of surface rotons on the vapor-liquid interface in liquid helium, which has been used to explain the observed temperature dependence of surface tension.[50]

The effect of thermal excitations localized in the neighborhood of an ion on the temperature dependence of its mobility has already been discussed in connection with the properties of the impurity mobility of anions (see Sec. B in Chap. 2). Analogous phenomena can, at least in principle, accompany the motion of ions in the roton gas. Qualitative estimates, reported by Bondarev[51] in connection with the role of localized rotons in the determination of the effective radius of a cation, confirm the reality of this effect.

Summarizing the foregoing survey, we may conclude that the development of a self-consistent theory of roton mobility of ions is not as yet complete.

3. OTHER TYPES OF MOBILITY

A. Stokes mobility

1) The hydrodynamic definition of the mobility of helium ions, which is valid for $l < R$ (l is the range and R is the ion radius), can be used in a broad temperature range for liquid He^3, in the neighborhood of the λ point in the case of superfluid helium, for which $\rho_s \ll \rho_n$, and for $T > T_\lambda$. Thus, to calculate the Stokes force acting on the ions, there is, in fact, no necessity to use the equations of two-fluid hydrodynamics, so that the initial predictions of the theory are very simple in this case. For bubbles, we have to consider the Stokes force calculated by Rybczynski (see[23], p. 91):

$$\mathbf{F}_- = 4\pi R_- \eta \mathbf{V}, \tag{3.1}$$

where $\mathbf{V}$ is the ion velocity and η is the first viscosity coefficient. For positive ions

$$\mathbf{F}_+ = 6\pi R_+ \eta \mathbf{V}, \tag{3.2}$$

where the effective radius R_+ is of the order of the Atkins radius.

The presence of the excess-density region around the cation means that we must consider the role of this region and of the second viscosity in the hydrodynamic mechanism of retarding of cations. The corresponding calculations, performed by Svidzinskiĭ,[52] yield the following expression for the additional force due to the increase in density:

$$\delta F_+ = F_+ \cdot \frac{2}{3} s \left[\frac{1}{13} - \frac{s}{259} \left(\frac{\zeta}{\eta} \right) \right], \quad s = \frac{\alpha e^2}{m_4 c_0^2 R_+^4}; \tag{3.3}$$

where F_+ is given by (3.2), α is the polarizability of helium, m_4 and c_0 are the mass of the He^4 atom and the velocity of sound in undisturbed helium, respectively, and ζ is the second viscosity of helium. In the case of helium, $s = 1/3$. It follows that, since the numerical coefficients are small, the additional force (3.3) can be neglected in mobility calculations.

Measurements of ionic mobility in the "Stokes region" performed by different authors[53] are shown in Fig. 18. According to these data, $\mu_\eta^+/\mu_\eta^- = 1.7$ at $T \approx 2.4°$. Using (3.1) and (3.2) together with this result, we can readily

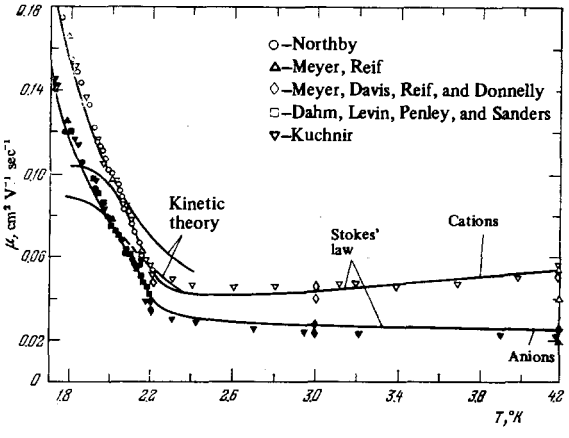

FIG. 18. Experimental data on the mobility of ions in the Stokes temperature region: Kuchnir,[53b] Meyer *et al.*[53c] The Meyer–Reif data on the roton mobility of ions are taken from[45a]. The other references to the experimental results in the roton region are given by Dahm and Sanders.[53a] Solid lines correspond to the Stokes definition of mobility, taking into account the viscosity data in[54a] and the data on the coefficient of surface tension in this temperature region.

9)The roton gap in homogeneous helium decreases with increasing pressure. Consequently, the region of excess pressure surrounding the cation should act as a potential well for the rotons.

show that $R_-/R_+ = 1.5 \times 1.7 = 2.5$, which corresponds to the "usual" helium ion radii $R_+ = 6-7$ Å and $R_- = 17-18$ Å.

The temperature dependence of $\mu_\eta^\pm$ in the region $T > 2$ °K is determined by the temperature dependence of the viscosity η [54a] and by the change in the bubble size with increasing temperature.

2) The relative simplicity of the description and the experimental conditions corresponding to the hydrodynamic region of the definition of mobility have stimulated various further experimental developments. One of these is the determination of the frequency dependence of mobility. Analysis of the equation of motion

$$M_\pm \left(\frac{dV}{dt} + \frac{V}{\tau_\pm} \right) = eE_0 e^{i\omega t}$$

shows that the imaginary part of the frequency dependence of mobility

$$\mathrm{Im}\,\mu^\pm(\omega) = \mu^\pm(0) \frac{\omega\tau_\pm}{1+(\omega\tau_\pm)^2}, \quad \mu^\pm(0) = \frac{e\tau_\pm}{M_\pm} \tag{3.4}$$

should have a maximum at $\omega\tau_\pm \sim 1$. By measuring the position of the relaxation maximum, i.e., by estimating the quantity $\tau_\pm$, and using the static mobility of a given ion for $\omega \to 0$, we can calculate the effective ion mass from the formula

$$M_\pm = \frac{e\tau_\pm}{\mu^\pm(0)}.$$

This was, in fact, the method used in the first measurement of the effective mass of the helium ion[53a] (Fig. 19). The precision of this method is, however, inferior to that attainable in the resonance method,[4,5] which was proposed later. Experiment shows that $M_\pm$ is a function of temperature. There is, as yet, no interpretation of this effect although, in the case of anions, it may be related to the change in R_- due to the temperature dependence of surface tension.

3) The variation of Stokes mobility of ions with increasing pressure was investigated by Keshishev *et al.*[55] It was expected to confirm the dependence of $R_\pm$ on pressure. In the case of positive ions, the Atkins radius is expected to vary with increasing pressure. If P and P_s denote, respectively, the external pressure and the solidification pressure of helium, the dependence

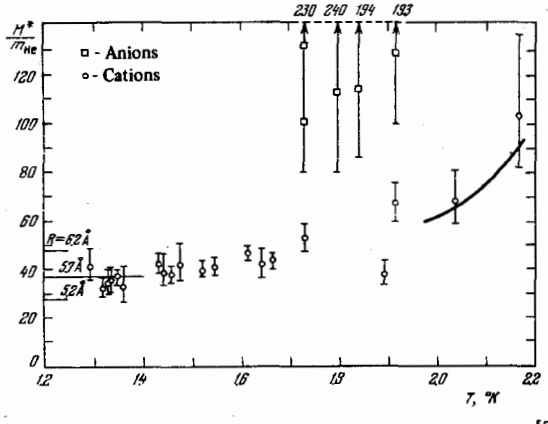

FIG. 19. Effective mass of helium ions obtained in[53a] from measurements of the frequency dependence of ion mobility.

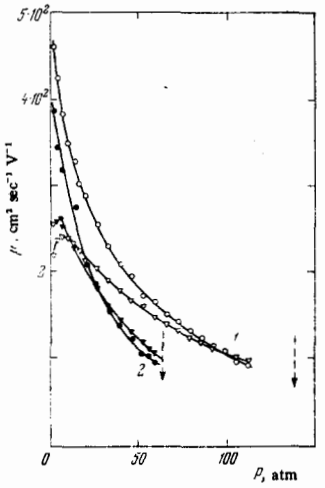

FIG. 20. Ion mobility in liquid helium as a function of pressure.[55] Open circles—cations; triangles—anions. Curves 1 and 2 were obtained at 4.2 and 2.63 °K, respectively. Arrows show the solidification pressure at the given temperatures. The curves clearly show the presence of maxima at $P \sim 10$ atm.

of R_+ on P has the form [compare this with (1.2)]

$$R_+^4 = \frac{\alpha e^2}{2\nu_4 |P - P_s|}. \tag{3.5}$$

As $P \to P_s$ we have $R_+ \to \infty$.

For anions, the imposition of an external pressure should lead to an initial reduction in the size of the bubble and, correspondingly, an increase in the anion mobility in the Stokes region (this effect must be distinguished from the effect of external pressure on the phonon mobility of ions discussed above; see Sec. A of Chap. 2). However, polarization forces subsequently come into play and the model is, roughly speaking, covered by a layer of solid helium so that the effective radius of the anion begins to increase with increasing pressure like R_+. As a result, the anion mobility as a function of applied external pressure should at first increase and then, having reached a certain maximum, fall again. A qualitative description of this type of nonmonotonic dependence of μ_η^- on P is described by Arkhipov in[2]. This effect and the change in R_+ with pressure has been confirmed experimentally.[55] The position of the maximum on the μ_η^- versus P curve is shown by Fig. 20, which is taken from[55], to occur at $P \sim 10$ atm. Finally, the expected dependence of R_+ on P, given by (3.5), occurs only at pressures that are not too high (see Fig. 21). For $P > 10$ atm, the experimental

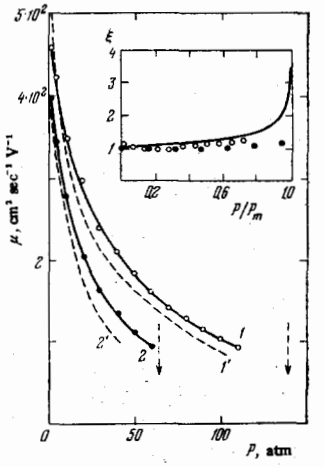

FIG. 21. Comparison of experimental mobility data with the calculated Stokes mobility in which R_+ is given by (3.4) and the viscosity is taken from[46b,55]. Solid lines—experiment: 1) $T = 4.2$ °K; 2) $T = 2.63$ °K. Dashed lines—theory. Insert shows the dimensionless quantity $\xi = R_+^4 \sqrt{2\nu_4 P_S/\alpha e^2}$ as a function of relative pressure.

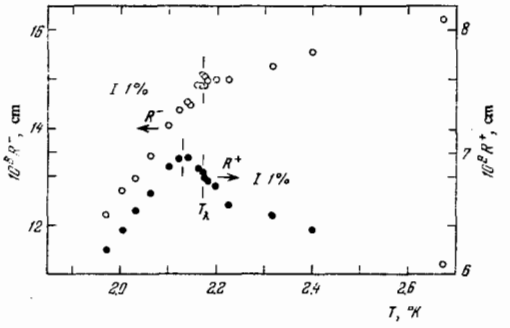

FIG. 22. R^+ and R^- as functions of temperature in the neighborhood of the λ point.[57]

dependence of R_+ on P is somewhat shallower than the theoretical prediction.

4) The temperature region immediately adjacent to T_λ deserves particular attention. The behavior of mobility in this temperature region has not as yet been investigated theoretically although it might be thought that the fact that the order parameter vanishes on the surface of the ion (this is the boundary condition for the Ginzburg–Pitaevskiĭ equation[56]) should lead to a deformation of the order parameter in the neighborhood of the ion and, consequently, to some observable effects on mobility. Experimental results obtained by Ahlers and Gamota[57] show that the radius of helium ions does, in fact, vary somewhat in the neighborhood of the λ point (Fig. 22). This conclusion is reached if, in addition to ionic mobility data, one uses independent measurements of the viscosity η of helium in the neighborhood of T_λ and expresses $R_\pm$ in terms of $\mu^\pm$ and η through the Stokes formulas

$$R_+ = \frac{e}{6\pi\eta\mu_\eta^+}, \quad R_- = \frac{e}{4\pi\eta\mu_\eta^-}.$$

The generally different behavior of R_- and R_+ in the region $T \gtrsim T_\lambda$, which is indicated by Fig. 22, has a simple explanation. The radius of the bubble is determined largely by the surface tension which decreases with increasing pressure. As a result, the radius R_- increases monotonically with increasing temperature, and a small anomaly δR_- appears against this background in the neighborhood of the λ point. So far as the radius R_+ is concerned, its variation near T is connected only with the proximity to the λ point. No such variations should occur well away from T_λ, and this is clear from Fig. 22. It is interesting to note that the maximum of R_+ is shifted somewhat relative to the λ point in the direction of lower temperatures. This fact is still unexplained.

B. Electron mobility in dense gaseous helium

The development of a quantitative theory of the mobility of electrons in the neighborhood of a critical gas concentration n_{crit}, sufficient for the appearance of electron bubbles in helium, is an interesting and complicated problem for the theory of unordered spectra. An account of the general results obtained by different workers in this area[58] would be a relatively difficult and laborious task. Nevertheless, without pretence to a description of mobility that would be valid throughout the intermediate region of gas concentrations, and approaching the critical region $n \sim n_{crit}$ from either direction, it is possible to determine the interaction of slow electrons with the fluctuating gas density in the language of the well-established theory of scattering of light and of slow neutrons in continuous media.

1) Suppose that $n < n_{crit}$. If, in addition,

$$\lambda \ll n^{-1/3}, \quad \lambda^2 \approx \frac{\hbar^2}{2m_e T} \tag{3.6}$$

where λ is the thermal-electron wavelength and m_e the electron mass, then we are dealing with the mobility of an electron in a gaseous medium. This mobility is given by[20]

$$\mu_e = \frac{3e}{32nf_0^2\sqrt{2\pi m_e T}}, \tag{3.7}$$

where f_0 is the scattering amplitude for an electron on an individual helium atom. For temperatures $T \sim 4$ °K, the inequality $\lambda \ll n^{-1/3}$ and the expression given by (3.7) are valid for $n \lesssim 10^{18}$ cm^{-3}.

The inequality given by (3.6) is violated as n increases. Under such conditions,

$$\lambda^{-3} < n < n'_{crit} \tag{3.8}$$

the concept of single-particle collisions loses its meaning, and we have to consider the character of the interaction of the electron with dense gaseous medium.

The proposed calculation of mobility is based on the following ideas. We shall write the interaction between electrons and the fluctuating medium in the form

$$\delta W_e = \frac{2\pi\hbar a_0}{m_e}\delta n, \tag{3.9}$$

which follows from (1.4), where δn is the density fluctuation. This interaction resembles the electron-phonon interaction in semiconductors, and may be used in the corresponding formalism for calculating the electron mobility if well-defined phonons of required wavelength are present in the gaseous helium.

Conservation laws that apply to the electron-phonon collision show that the maximum phonon wave numbers q_{max} contributing to electron scattering are of the order

$$q_{max} \approx 2k, \tag{3.10}$$

where k is the characteristic electron wave number. In very weak electric fields, when there is no appreciable heating of the electron gas, the electron temperature is equal to the temperature of the gaseous medium, i.e., as already noted, $k \lesssim 10^6$ cm^{-1} for $T \sim 4$–5 °K. Consequently, phonons participating in the slowing down of electrons should have wave numbers $q_{max} \lesssim 10^6$ cm^{-1}. The region in which such waves exist is restricted in the short-wave limit by wavelengths of the order of the mean free path of the gas atom.[35] In gaseous helium, the characteristic mean path l of the gas atoms is of the or-

der of a few interatomic distances, i.e., $l \gtrsim 10^{-6}$ cm for $n \sim 10^{19}$ cm^{-3}. Consequently, the maximum wave numbers of acoustic phonons under the conditions in which we are interested are of the order of $q_{max} \sim 10^6$ cm^{-1}, and this agrees in order of magnitude with the scale of q_{max} necessary for (3.10) to be satisfied. This agreement means that the electron-phonon interpretation of the interaction (3.9) is reasonable. The dispersion relation for the corresponding gas phonons is

$$\omega = cq, \quad c^2 = \frac{c_p T}{c_v m_4}, \tag{3.11}$$

where c_p/c_v is the ratio of specific heats. For helium, $c_p/c_v = 1.66$.

Calculations of the electron-phonon mobility of electrons in a gas differ from the analogous calculations for semiconductors only in the meanings of the constants of the theory. We shall not, therefore, reproduce the derivation and merely quote the final expression[59]:

$$\mu_e = \frac{9}{8\pi} \frac{(c_p/c_v)\, e}{n a_0^2 \sqrt{m_e T}}. \tag{3.12}$$

This expression is practically identical with (3.7). The only difference is in the values of the numerical coefficients and in the interpretation of the scattering cross sections. Whereas, in (3.7), we were concerned with single-particle s scattering of an electron by an individual He^4 atom, in (3.12) the quantity a_0 is an effective scattering length which arises in the optical model of the interaction between the low-energy electron and the dense gaseous medium. This similarity is the main reason for the fact noted in[11] that the formula given by (3.7) provides a sufficiently good description of the mobility of electrons in gaseous helium right up to $n \lesssim 5 \times 10^{20}$ cm^{-3}. It is clear that the basic condition $\lambda \ll n^{-1/3}$ has long been violated in this region and, in fact, we have to consider the agreement of experimental data with (3.12) and not (3.7).

2) In the opposite limiting case, i.e., $n > n_{crit}$, the electrons tend to localize, and the "depth" δ of a localized electron level relative to the energy of the electron in the unlocalized state begins to exceed the temperature quite appreciably. We then have the possibility of the subsivision of the electrons introduced into helium into localized electrons with concentration n_i and free electrons with concentration n_e. In thermodynamic equilibrium, the chemical potentials of localized and free electrons should be equal, and this is the basis for the following expression for the relative concentration of localized electrons:

$$\frac{n_e}{n_i} = \left(\frac{m_e}{M_i}\right)^{3/2} \exp\left(-\frac{\delta F_0}{T}\right); \tag{3.13}$$

where M_i is the effective mass of an anion in the gas which is equal to the associated mass of the bubble, $M_i \approx (2/3)R_*^3 \rho$, and ρ is the density of helium. The quantity δF_0 is taken from the numerical calculations described in Chap. 1 [see Eq. (1.13)], or is obtained by solving the model problem on the localization of an electron in dense helium in which the helium density distribution is approximated by a rectangular and spherically symmetric well.[60]

Using (3.13) and introducing the idea of an effective mobility of electrons in gaseous helium through the expression

$$\mu^* = \left(1 - \frac{n_e}{n_i}\right)\mu_i + \frac{n_e}{n_i}\mu_e, \quad \mu_i = \frac{e}{4\pi\eta R_-}, \tag{3.14}$$

we can compare μ^* with existing experimental data on electron mobility in dense gas (see Fig. 2). In the above expressions, μ_e is given by (3.12) and η is the first viscosity coefficient of the gas. This type of comparison establishes an important fact which enables us to improve quite substantially the position of the critical density n_{crit} in Fig. 2. The point is that the observed result is $\mu_e/\mu_i \sim 10^5$. At the same time, according to (3.13), the ratio n_e/n_i should be of the order of 10^{-7} even for $\delta F_0/T \sim 1$ because of the large difference between the masses m_e and M_i which is of the order of $100 m_{He^4}$.

The final result is that, in the region of self-localization of electrons, the effective mobility μ^* given by (3.14) is practically equal to μ_i and, consequently, is a relatively slowly-varying function of n. This, however, means that n_{crit} should lie in the lower part of the transition region on the $\mu^*(n)$ graph, where the dependence of μ^* on n exhibits the asymptotic Stokes behavior. All this is well correlated with the calculated value $n_{crit} \approx 2 \times 10^{21}$ cm^{-3} obtained in Chap. 1, Sec. C.

It is important to note that agreement between calculations and measured values of μ^* was achieved in[58] throughout the intermediate region of values of n. However, an account of these results would require the introduction of a series of special definitions from the theory of unordered spectra and from percolation theory (see, for example, the review given in[61]), which lie outside the scope of the present review.

3) As noted in Chap. 1, the introduction of a strong magnetic field leads to the appearance of large-radius anions for $n < n_{crit}$. These take the form of ellipsoids of revolution, highly elongated along the magnetic field and producing a small perturbation on the initial gas density. The size of the large-radius anion for $n \lesssim 10^{21}$ cm and $H \lesssim 10^6$ G is appreciably greater than the mean free path of the gas atoms at comparable densities and temperatures ($r_0 \approx 3 \times 10^{-7}$ cm, $R_z \approx 8 \times 10^{-7}$ cm, and $l \approx 10^{-7}$ cm). As a result, we can use the hydrodynamic approximation in estimates of the mobility of large-radius anions in the direction of the magnetic field.

The motion of the variable-density region in the direction of the magnetic field with velocity V leads to the appearance of a velocity field which can be determined from the equations

$$\operatorname{div} \mathbf{v} = -\frac{V}{T}\frac{\partial \psi}{\partial z}, \quad \operatorname{rot} \mathbf{v} = 0, \tag{3.15}$$

where $\psi(r, z)$ is given by (1.10a) in Chap. 1.

If we know the field $\mathbf{v}$, we can calculate the energy dissipation $\dot{W}$ in the viscous fluid, using existing hydro-

dynamic formulas. On the other hand, the work done by the guiding electric field per unit time during the motion of the ion with constant velocity V is eEV. The equation $eEV = \dot{W}$ will define V and hence the mobility of the large-radius anion[12]:

$$\mu_H = \frac{e}{6\pi\eta R^*}, \quad R^* \approx 0.5\,(\gamma r_0)^2 R_i^{-1}, \tag{3.16}$$

where γ is given by (1.15). The quantity μ_H obtained under the conditions defined by (1.16a), is lower by two or three orders of magnitude than the mobility of free electrons at the same gas density and temperature.

Large-radius anions have not as yet been observed.

C. Mobility in solid helium

The ambiguity in the definition of the structure of helium ions in solid helium, noted in Chap. 1, forces us to consider the various ways in which charges can be transported through the helium lattice. For charges in the form of point defects, this may involve different modifications of the hopping mechanism in which the motion of a charge through the lattice is achieved by successive hops through the interatomic distance. If, on the other hand, the ion is a macroscopic formation (for example, a bubble of radius ~ 10 Å), its motion through the lattice is probably of the viscous diffusion or plastic origin.

1) Mobility of charged point defects

Experimental studies of the diffusion of point defects in solid helium (we have in mind the diffusion of He^3 atoms in an He^4 host and spin diffusion in solid He^3) have established that the displacement of such defects through the helium lattice occurs largely through the use of vacancies in the original host matrix. In other words, the most probable process determining the diffusion coefficient for a point impurity in helium is a hop to a neighboring site as soon as the site becomes vacant. Detailed arguments in favor of this mechanism of diffusion are given in a recent review by Andreev.[62] Since this review gives a complete description of the situation in the study of quantum diffusion of uncharged defects

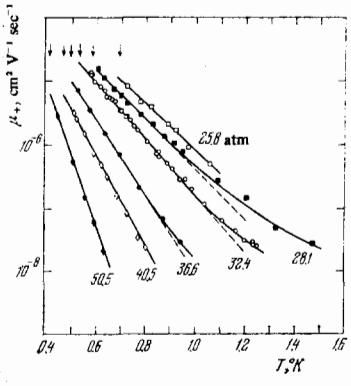

FIG. 23. Temperature dependence of the mobility of cations in hcp He^4 at different pressures.[64] Arrows show the melting points corresponding to these pressures.

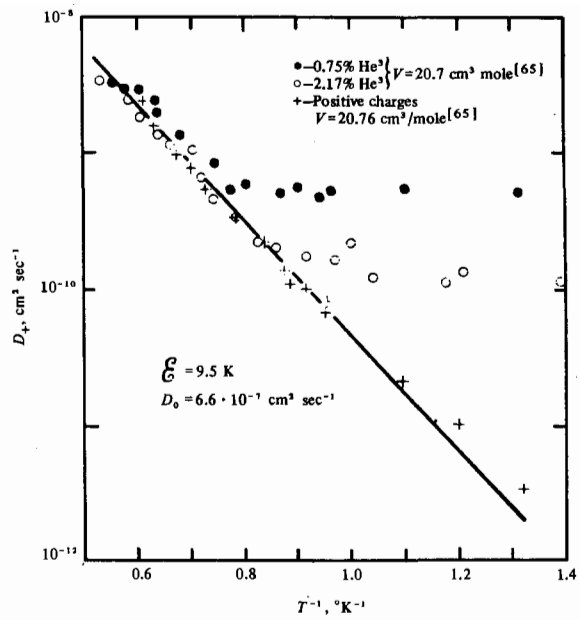

FIG. 24. Temperature dependence of the cation diffusion coefficient D_+ and He^3 atoms in hcp He^4.[64] $D_+ = D_0 \exp(-\mathcal{E}/T)$.

in solid helium, we shall confine our attention to certain properties of the mobility of charged point defects as compared with uncharged defects.

The mobility of cations in solid helium, and these cations are undoubtedly charged point defects, has been measured by different methods by various workers.[15,16,63,64] The results of the most recent and most careful measurements of cation mobility in solid He^4 were carried out by Kishishev and Shal'nikov[64] and are shown in Fig. 23. Moreover, Fig. 24 shows the experimental data on the cation diffusion coefficient D_+ and the He^3-atom diffusion coefficient D_3 in the He^4 lattice for equal molar volumes and temperatures. The data on D_3 are taken from[65]. The results shown in Figs. 23 and 24 lead to the following conclusions: a) the diffusion coefficients D_3 and D_+ are practically equal in the thermal activation region; b) as the temperature is reduced, the He^3 atoms lose their localization and begin to tunnel through the lattice, and c) no tendency toward delocalization is observed for cations.

The difference between the behavior of D_3 and D_+ at low temperatures can readily be explained by recalling that the charged impurity will interact with the lattice more intensively than an uncharged impurity. We are, of course, concerned here with the polarization interaction between the lattice atoms and the point charge, which gives rise to a local deformation of the lattice in the charge localization neighborhood. A similar interaction in liquid helium leads to the appearance of a spherical solidified-helium region (Atkins sphere) around the bare positive charge. In this case, the polarization interaction reduces sharply the probability of cation tunneling through the solid helium lattice, as compared with an uncharged point impurity and this has been confirmed experimentally.

The existence of the strong polarization interaction between a charge and the lattice atoms might be ex-

pected to give rise to an appreciable change in the energy of the interaction between the vacancy and the charged defect, so that the above difference between D_+ and D_3 at low temperatures should continue into the thermal-activation region. In reality, this is not so. The point is that the effective interaction V_v^+ between the charge and the vacancy is determined by the sum of two interactions, namely,

$$V_v^+ = V_\alpha(r) + V_\sigma(r), \quad V_\sigma = \omega_{ik}\sigma_{ik}, \tag{3.17}$$

where V_α is the direct interaction between the vacancy and the charge, which is repulsive (the helium atom is attracted to the charge due to polarization forces and, correspondingly, the vacancy should be repelled by the same charge with the same strength), so that the interaction V_σ appears as a result of the presence of an additional elastic deformation of polarization origin around the charge. The second term is given by $V_\sigma = \omega_{ik}\sigma_{ik}$, where σ_{ik} are the elastic stresses due to polarization forces and ω_{ik} is the change in the lattice volume due to the presence of vacancies in it. In the special case of an isotropic elastic medium, we have $\omega_{ik} - \omega_v\delta_{ik}$, and the expression for V_σ assumes the form $V_\sigma \approx \omega_v\sigma_{ii}$. In the case of a vacancy, the quantity ω_v is usually assumed to be negative,[88] so that the components V_α and V_σ of the resultant interaction V_v^+ have different signs. Since the two components of (3.17) have the same coordinate dependence, i.e., $V_\alpha \propto V_\sigma \propto r^{-4}$, it is readily verified that, for reasonable values $\omega_v^+ \sim a^3$ (a is the interatomic distance), strong compensation of one term by the other is possible, and

$$V_v^+ = \frac{1}{2}\frac{\alpha e^2}{r^4}\left[1 - \omega_v n\frac{(3-5\sigma)}{(1-\sigma)}\right], \tag{3.17a}$$

where α is the atomic polarizability of helium, n is the mean density of atoms in the solid helium lattice, and σ is the Poisson ratio. When

$$\left[1 - \omega_v n\frac{(3-5\sigma)}{(1-\sigma)}\right] \to 0 \tag{3.18}$$

we have $V_v^+ \to 0$ and, consequently, the thermal-activation diffusion coefficient for cations, D_+, which is of vacancy origin, will not be different from the diffusion coefficient D_3 in this region.

It is important to note that the possibility of strong renormalization of the interaction V_v^+ between the cation and the vacancy is analogous to the renormalization of the interaction V_3^+ between impurity excitations and cations in weak solutions of He^3 in He^4 [see the definition of V_3^+ given by (2.10) and the discussion of this]. The difference is only that, in the case of cation mobility in weak liquid He^3–He^4 solutions, the degree of compensation is known from independent measurements. The theory of cation mobility in weak He^3–He^4 solutions can therefore provide quantitative predictions on the magnitude of μ_3^+ and its temperature behavior. In the case of cation mobility in solid helium, the quantity ω_v or, more precisely, ω_{ik} is not as yet known. It follows that the possibility of strong renormalization can only by hypothesized, and the scale of ω_v can be determined with the aid of (3.18).

The observed properties of the temperature dependence of the cation mobility in solid helium (as compared with the mobility of uncharged point impurities at similar temperatures and pressures) can thus be reasonably explained in a qualitative fashion.

2) Diffusion mobility of anions

2.1. *Stationary mobility.* One of the possible mechanisms for the mobility of a macroscopic anion in solid helium is of diffusion origin.[18] An electron in a spherical cavity begins to exert asymmetric pressure on the bubble walls when an external electric field E is applied. After a certain transient period, this pressure leads to the appearance of stationary diffusion currents of vacancies from regions with enhanced pressure to points with reduced pressure. The existence of such currents is, in fact, responsible for the motion of the bubble as a whole in the direction of the guiding field E. Diffusion problems of this type have already been encountered (see, for example,[87]) in the case of the viscous-diffuse flow of polycrystals under the action of external pressure. The necessary set of equations and its derivation can therefore be taken over as they stand from such work.

The stationary volume vacancy field $c(\mathbf{r})$ is described by the harmonic equation[10)]

$$\Delta c = 0 \tag{3.19}$$

subject to the boundary condition

$$c|_{r=R_-} = \frac{c_s\omega_v}{T}\delta P_n, \tag{3.20}$$

where P_n is the normal pressure on the surface of the ion of radius R_-, c_s is the equilibrium concentration of vacancies on the surface of the ion, ω_v is the volume of one vacancy, and T is the temperature. The normal currents of vacancies on the surface of the ion determine the local velocity $V_n(\theta)$ of an element of the anion surface:

$$D_v\frac{\partial c}{\partial r}\Big|_{R_-} = V_n(\theta), \tag{3.21}$$

where D_v is the vacancy diffusion coefficient.

The condition $V_n(\theta) = V_0\cos\theta$, where V_0 is the velocity of the ion as a whole, will ensure that the ion will move as one whole without deformation. Having thus determined the pressure on the surface of the ion, and having solved the harmonic problem defined by (3.19)–(3.21), we can relate V_0 to the applied electric field, i.e., determine the mobility of the ion $\mu = V_0/E$.

The electron pressure on the surface of the ion, δP_{el}, can be obtained from formulas similar to (2.7) in which $\psi(r, \theta)$ is the solution of the Schrödinger equation

[10)] We are neglecting surface diffusion over the surface of the ion because the surface layer of the ion is under high spherically symmetric electron pressure, so that surface diffusion cannot appreciably exceed volume diffusion.

for the electron in a spherical potential well, specified by the boundary condition $\psi(r,\theta)|_{R_-}=0$, in the presence of the perturbing electric field E.

The resulting formula for δP_{el} is given by the following order-of-magnitude expression:

$$\delta P_{el} \approx P_{el}^0 \frac{eER_-}{W}\cos\theta, \quad P_{el}^0 = \frac{W}{\omega_i}, \tag{3.22}$$

where W is the energy of the electron in the ground state, P_{el}^0 is the spherically symmetric pressure of the electron on the surface of the bubble, and ω_i is the volume of the bubble.

Using the relation between E and δP_{el}, and solving the set of equations (3.19)–(3.21), we can readily obtain the expression for the mobility of the charged bubble:

$$\mu_s^- = \frac{V_0}{E} = c_s \frac{\omega_v}{\omega_i}\frac{eED_v}{T}. \tag{3.23}$$

To define the mobility μ_s^- given by (3.23) fully, we must elucidate the significance of c_s. In the general case of an anisotropic elastic medium, the concentration of vacancies on the surface of the charged spherical cavity in solid helium may be different from the equilibrium concentration $c_0(T)$ well away from the anion. However, in the approximation of an isotropic elastic medium, and using the considerations leading to (3.17a) as a representation of the interaction between the point charge and the vacancy, we find that the concentration of vacancies on the surface of the bubble is the same as the volume concentration, i.e., $c_s(T) \approx c_0(T)$.

2.2. *Mobility in alternating field.* We recall that the high-frequency mobility of ions in liquid helium contains a number of relaxation peaks (3.4), the positions of which enable us to estimate the relaxation time and the effective mass of helium ions in liquid helium. Analogous peaks on the frequency dependence of mobility should be observed for ions in solid helium. It is only their particular positions that are determined by other parameters.

The problem of the frequency dependence of the mobility of negative ions in solid helium is formally different from the set of equations (3.19)–(3.21) in that (3.19) is replaced by the diffusion equation

$$i\omega c = D_v \Delta c. \tag{3.24}$$

It is readily shown, by solving this set of equations, that

$$\operatorname{Im}\mu_s^-(\omega) = \mu_s^-(0)\frac{x}{(1+x)^2+x^2}, \quad x = \frac{\omega R_-^2}{2D_v}. \tag{3.25}$$

This is completely analogous to (3.4) and indicates the existence of a relaxation maximum at frequency $\omega \approx \sqrt{2}D_v/R^2$.

2.3. *Some quantum features of mobility.* The mobility of ions in solid helium is interesting not only in itself. There is added interest in connection with the possibility of being able to investigate the properties of defects in the solid helium lattice with the aid of charged particles. For example, Andreev and Lifshits[68] have discussed in a general way the possible existence in solid helium of vacancies of quantum origin, which have a nonzero concentration as $T \to 0$. In addition, even at sufficiently high temperatures, helium vacancies should lose their localization and transform into quasiparticles, i.e., "vacancions." All these features of the behavior of vacancies have a direct relationship to the mobility of negative ions.

As the temperature is reduced, calculations of the mobility of anions must, first of all, be corrected for the loss of localization by the vacancies. According to Pushkarov's estimates,[69] the mean free path of vacancies becomes appreciably greater than the interatomic distance for temperatures $T < T_D/8$, i.e., for $T \lesssim 1$ °K. The relationship between the boundary values of the excess concentration of vacancies and the pressure on the surface of the ion is still of the classical form in this case, i.e.,

$$\delta c(R_-) = \frac{c_s v_v}{T}\delta P_{el}.$$

However, the spatial distribution of the vacancies and the corresponding vacancy currents must now be determined with the aid of the diffusion equation and not from the solution of the kinetic equation for the vacancy distribution function.

Details of these calculations are given in[18]. Here we merely reproduce the final expression for the velocity of the ion under these conditions:

$$V_0 = c_s \frac{eER_-}{T}\frac{\omega_v}{\omega_i}\sqrt{\frac{T}{2\pi m^*}}, \quad \omega_i = \frac{4}{3}\pi R_-^3, \tag{3.26}$$

where m^* is the effective mass of the "vacancion" and R_- is the ion radius. This result is qualitatively different from the diffusion formula given by (3.23) and has a simple physical interpretation. When the "vacancions" freely approach and leave the surface of the ion, the velocity of the ion as a whole is limited by only two factors, namely, the concentration of nonequilibrium vacancies on the ion surface, which can be estimated from

$$\delta c \approx c_s \frac{eER_-}{T}\frac{\omega_v}{\omega_i},$$

and the rate of escape (arrival) of vacancies on the surface, i.e., the thermal velocity of vacancies $v_T \approx (2T/m^*)^{1/2}$. As a result, $V_0 \approx v_T \delta c$, which is also predicted by (3.26).

It is clear that the result given by (3.26) is valid provided $T \ll \Delta_v$, where Δ_v is the width of the "vacancion" band (it is suggested in[62] that $\Delta_v \sim 1$ °K). If, on the other hand, the temperature of the medium is higher than Δ_v, the characteristic velocity of the "vacancion" is given by $v \sim a\Delta_v\hbar^{-1}$. Correspondingly, the diffusion coefficient D_- and the anion mobility μ_s^- assume the form

$$D_- \sim c_0(T)\Delta_v a^2\hbar^{-1}\left(\frac{a}{R_-}\right)^2, \quad \mu_s^- = \frac{eD_-}{T}, \tag{3.26a}$$

provided $c_s(T) \approx c_0(T)$, where $c_0(T)$ is the equilibrium concentration of vacancies, $c_0(T) = c_0\exp(-\mathscr{E}/T)$, and $\mathscr{E}$

is the vacancy activation energy. Comparing D_- as given by (3.26) and (3.26a) with the definition of D_3 or D_+ in the thermal-activation region, as given in[62], we obtain

$$D_3 \sim D_+ \sim \begin{cases} c_0\sigma_{in}\hbar^{-1}\Delta_v, & T \gg \Delta_v; \\ c_0\sigma_{in}\hbar^{-1}\sqrt{\Delta_v T}, & T \ll \Delta_v, \end{cases} \qquad (3.27)$$

where σ_{in} is the cross section for the inelastic scattering of a "vacancion" by a point defect (by definition,[62] an inelastic scatter is the collision between a defect and a vacancy accompanied by a hop of the defect through the interatomic distance; in the second limiting case, $T \ll \Delta_v$, we use $v \sim \sqrt{T/m^*}$, $m^* \sim \hbar^2/a^2\Delta_v$), and it may be concluded that

$$\frac{D_+}{D_-} \sim \frac{\sigma_{in}}{a^2}\left(\frac{R_-}{a}\right)^2. \qquad (3.28)$$

2.4. *Measurements of the mobility of anions* in solid He^4 have been carried out in the most complete form by Kishishev and Shal'nikov.[64] The measured mobilities reported in[64] as functions of temperature and pressure are collected together in Fig. 25. In addition, Fig. 26 shows the activation energies $\mathscr{E}$ for the cation and anion mobility as functions of the molecular volume of solid hcp He^4.

Comparison of experimental data shown in Figs. 23, 25, and 26 enabled us to conclude that for pressures $P \gtrsim 40$ atm, the cation and anion mobilities are practically equal. This could be regarded as a demonstration of the absence of bubbles with $R_- \gg a$ in solid helium if the quantity σ_{in} in the expression given by (3.27) for D_+ were of the order $\sigma_{in} \sim a^2$. In reality, however, the true value of σ_{in}, determined with the aid of (3.27) and the data in Fig. 23, turns out to be much smaller, i.e., $\sigma_{in} \lesssim 10^{-1}a^2$.[11)] For this low value of the cross section for the scattering of a vacancy by a point defect, the observed numerical equality of D_+ and D_- is, according to (3.28), equivalent to $(R_-/a)^2 \gtrsim 10$. This inequality is not inconsistent with $R_- \gg a$, i.e., it cannot be used as an argument in favor of the point structure of anions in solid helium.

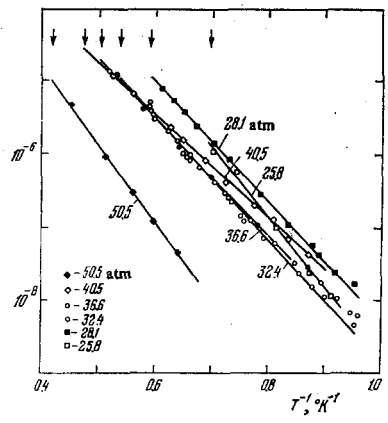

FIG. 25. Temperature dependence of the mobility of anions in hcp He^4 for different pressure.[64] Arrows show the melting points at the corresponding pressures.

At low pressures, $P < 40$ atm, the behavior of cations and anions is known to be different. According to Fig. 23, the cation mobility increases monotonically as the pressure is reduced. The mobility of anions (Fig. 25) at first increases with decreasing pressure, then passes through a maximum and, finally, falls again for $P \ll 40$ atm. A similar difference between the cation and anion mobilities as functions of pressure is observed in liquid helium (see Fig. 20 and a discussion in text). However, in the case of solid helium, the interpretation of this difference is very much less clear. The anomalous behavior of the activation energy for the anion mobility at low pressures (Fig. 26) is of particular interest. The bubble model of an anion suggests a possible origin for this behavior of the activation energy.

The solution of the equilibrium problem for an elastic medium with a spherical cavity of radius $R_- \gg a$ containing a localized electron in the presence of an isotropic compressive pressure P_∞ at infinity yields

$$\sigma_{rr} = P_\infty\left(1 + \frac{R_-^3}{r^3}\frac{P_l + P_\alpha}{P_\infty}\right),$$
$$\sigma_{\theta\theta} = \sigma_{\varphi\varphi} = P_\infty\left(1 - \frac{R_-^3}{2r^3}\frac{P_l + P_\alpha}{P_\infty}\right),$$

where P_l and P_α are the Laplace and polarization pressures on the surface of the bubble (polarization forces are, in general, distributed throughout the volume of the elastic medium but, in the case of the determination of the effective radius of the bubble, they can be replaced by the equivalent pressure on the surface of the bubble. The radius R_- is obtained from the condition $P_{el} = P_\infty$

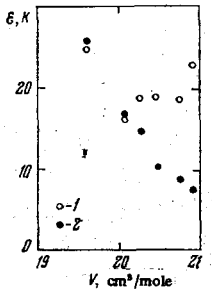

FIG. 26. Activation energy for anion (1) and cation (2) mobilities as functions of molar volume of solid He^4.[64]

[11)] If $\Delta_v \leq 1$ °K and is a slowly varying function of pressure (according to the calculations of Mineev,[70] a change in the molar volume of hcp He^4 within the range 20.23 – 18.23 cm^3/mole gives rise to a change in Δ_v within the range $1 \lesssim \Delta_v \lesssim 1.5$ °K), then if we use the first of the asymptotic expressions in (3.27) and the data in Fig. 23, we find that, for pressures between 21.8 and 50.5 atm, the cross section σ_{in} is an increasing function of pressure and assumes values in the range $5\times10^{-3}a^2 \lesssim \sigma_{in} \lesssim 5\times10^{-1}a^2$, $a \approx 3.5$ Å.

In the other limiting case, when $\Delta_v > 1$ °K (the basis for this limiting case is the numerical value $\Delta_v \approx 4$–5 °K, obtained by Keshishev and Shal'nikov[64] in the interpretation of experimental data on effects in the motion of charges through solid helium, which are nonlinear in the electric field), we would have to use the second asymptotic formula in (3.27) to interpret the experimental data in Fig. 23. As a result, the cross section σ_{in} at the same pressures turns out to be somewhat lower: $10^{-3}a^2 \lesssim \sigma_{in} \lesssim 10^{-1}a^2$. It is important to note that, in the second method of analyzing the pre-exponential factors in the graphs of Fig. 23, the results for σ_{in} are practically independent of the temperature (as expected), whereas, in the first variant, the cross section is temperature-dependent.

$+P_i+P_\alpha$. As a result, an elastic stress field $\sigma_{ik}(r)$ appears around the charged spherical cavity, which depends on r and has the property $\sigma_{ii}=3P_\infty$. Consequently, within the framework of the theory of isotropic elastic media, the energy of a vacancy in the neighborhood of a charged bubble, V_σ, written in the form of $V_\sigma=\omega_v\sigma_{ii}$, is independent of the coordinates. However, since, in reality, we are dealing not with an isotropic elastic medium or a cubic crystal (we are interested in solid He^4 with a hcp lattice), the general expression $V_\sigma=\omega_{ik}\sigma_{ik}$ may turn out to be a function of the coordinates and, by definition, have a minimum at $r=R_-$. The surface concentration of vacancies on the boundary of the bubble will then be given by

$$c_s=c_0(T)\exp\left[\frac{V_\sigma^*(R_-)}{T}\right],\quad V_\sigma^*=\omega_{ik}(\sigma_{ik}-3P_\infty\delta_{ik}),$$

i.e., it will differ exponentially from the equilibrium concentration of vacancies c_0. The presence of enhanced concentration of vacancies on the surface of the bubble, which increases exponentially with increasing pressure at infinity, must, of course, be compared with observed anomalies in the behavior of activation energy for anion mobility.

The author is indebted to A. F. Andreev and L. P. Mezhov-Deglin for numerous discussions of the problems raised in this review and to K. O. Kishishev for placing at his disposal experimental data on the mobility of ions in solid helium, which were part of his thesis.

[1]K. R. Atkins, Phys. Rev. **116**, 1339 (1959).
[2]R. G. Arkhipov, Usp. Fiz. Nauk **88**, 185 (1966) [Sov. Phys. Usp. **9**, 174 (1966)].
[3]E. P. Gross, Ann. Phys. (N.Y.) **19**, 234 (1962).
[4]V. B. Shikin, Zh. Eksp. Teor. Fiz. **58**, 1748 (1970) [Sov. Phys. JETP **31**, 936 (1970)].
[5]J. Poitrenaud and F. J. B. Williams, Phys. Rev. Lett. **29**, 1230 (1972); **32**, 1213 (1974).
[6]R. A. Ferrel, Phys. Rev. **108**, 167 (1957).
[7]G. Careri, V. Fasoli, and F. Gaeta, Nuovo Cimento **15**, 774 (1960).
[8]W. T. Sommer, Phys. Rev. Lett. **12**, 371 (1964).
[9]a) B. Halperin and R. Gomer, J. Chem. Phys. **43**, 1069 (1965); I. A. Gachechiladze, K. O. Keshishev, and A. I. Shal'nikov, Pis'ma Zh. Eksp. Teor. Fiz. **12**, 231 (1971) [JETP Lett. **12**, 159 (1971)]; V. N. Lebedenko and B. U. Rodionov, Pis'ma Zh. Eksp. Teor. Fiz. **16**, 583 (1972) [JETP Lett. **16**, 411 (1972)]; L. Bruschi, G. Mazzi, and M. Sautini, Phys. Rev. Lett. **28**, 1504 (1972); R. J. Loveland, P. G. Le Comber, and W. E. Spear, Phys. Lett. A **39**, 225 (1972). b) K. F. Canter, J. D. McNutt, and L. O. Roelling, Phys. Rev. A **12**, 375 (1975).
[10]B. E. Springett, M. H. Cohen, and J. Jortner, Phys. Rev. **159**, 183 (1967); Yu-Min Shih and Chia-Wei Woo, Phys. Rev. A **8**, 1437 (1973).
[11]K. L. Levin and T. M. Sanders, Phys. Rev. **154**, 138 (1967).
[12]L. S. Kukushkin and V. B. Shikin, Zh. Eksp. Teor. Fiz. **63**, 1830 (1972) [Sov. Phys. JETP **36**, 969 (1973)].
[13]A. G. Khrapak and I. T. Yakubov, Teplofiz. Vys. Temp. **11**, 1115 (1973).
[14]H. R. Harrisson and B. E. Springett, Phys. Lett. A **35**, 73 (1971).
[15]K. O. Keshishev, L. P. Mezhov-Deglin, and A. I. Shal'nikov, Zh. Eksp. Teor. Fiz. **12**, 234 (1970) [Sov. Phys. JETP **12**, 160 (1970)].
[16]G. A. Sai-Halasz and A. J. Dahm, Phys. Rev. Lett. **28**, 1244 (1972).
[17]M. H. Cohen and J. Jortner, Phys. Rev. **180**, 238 (1969).
[18]V. B. Shikin, Zh. Eksp. Teor. Fiz. **61**, 2053 (1971) [Sov. Phys. JETP **34**, 1095 (1972)].
[19]A. F. Andreev and A. É. Meĭerovich, Zh. Eksp. Teor. Fiz. **67**, 1559 (1974) [Sov. Phys. JETP **37**, 829 (1974)].
[20]B. M. Smimov, Usp. Fiz. Nauk **92**, 75 (1967) [Sov. Phys. Usp. **10**, 313 (1967)].
[21]H. T. Davis and R. Dagonnier, J. Chem. Phys. **44**, 4030 (1966).
[22]G. Baym, R. Barrera, and C. Pethich, Phys. Rev. Lett. **22**, 20 (1969).
[23]L. D. Landau and E. M. Lifshitz, Mekhanika sploshnykh sred (Mechanics of Fluids), Moscow, Gozdakhizdat, 1953 (Pergamon Press, Oxford, 1959).
[24]K. W. Schwarz and P. W. Stark, Phys. Rev. Lett. **22**, 1278 (1969).
[25]V. B. Shikin, Abstract of Theisi, Kharkov, 1974.
[26]K. W. Schwarz and P. W. Stark, Phys. Rev. Lett. **21**, 967 (1968).
[27]E. P. Gross and H. Tung-Li, Phys. Rev. **170**, 253 (1968); V. Celli, M. H. Cohen, and M. J. Zuckerman, Phys. Rev. **173**, 253 (1968).
[28]P. M. Morse and H. Feshbach, Methods of Theoretical Physics, McGraw-Hill, New York, 1953 (Russ. Transl., Vol. 2, IL, M., 1958, p. 463).
[29]a) R. M. Ostermeier, Phys. Rev. A **8**, 514 (1973); b) B. E. Springett, Phys. Rev. **155**, 139 (1966); c) C. Zipfel and T. M. Sanders Jr., in: Proc. Eleventh Intern. Conf. on Low-Temperature Physics, ed. by J. F. Allen *et al.*, University of St. Andrews, Scotland, 1969, p. 296.
[30]a) B. N. Esel'son, Yu. Z. Kovdrya, and V. B. Shikin, Zh. Eksp. Teor. Fiz. **59**, 64 (1970) [Sov. Phys. JETP **32**, 37 (1971)]; b) D. A. Neeper and L. Mayer, Phys. Rev. **182**, 223 (1969); c) L. Meyer and F. Reif, Phys. Rev. Lett. **5**, 1 (1960).
[31]M. Kuchnir, J. B. Ketterson, and P. R. Roach, Proceedings of the 12th Int. Conf. on Low Temperature Physics, Academic of Japan, Kyoto, 1971, p. 105; Phys. Rev. A **6**, 341 (1972).
[32]J. Bardeen, G. Baym, and D. Pines, Phys. Rev. **156**, 207 (1967).
[33]R. M. Bowley and J. Lekner, J. Phys. C **3**, L127 (1970).
[34]T. F. O'Malley, L. Spruch, and L. Rosenberg, J. Math. Phys. **2**, 491 (1961).
[35]L. Boltzmann, Lectures on the Theory of Gases, California, University Press, 1964 (Russ. Transl. from German, Gostekhizdat, M., 1963, p. 244).
[36]A. F. Andreev, Zh. Eksp. Teor. Fiz. **50**, 1415 (1966) [Sov. Phys. JETP **23**, 939 (1966)].
[37]V. B. Shikin, Zh. Eksp. Teor. Fiz. **64**, 1414 (1973) [Sov. Phys. JETP **37**, 718 (1973)].
[38]L. D. Landau and E. M. Lifshitz, Statisticheskaya fizika (Statistical Physics), Moscow, Nauka, 1964 (Pergamon Press, Oxford, 1975).
[39]V. I. Mel'nikov, Zh. Eksp. Teor. Fiz. **63**, 696 (1972) [Sov. Phys. JETP **36**, 368 (1973)].
[40]H. Gould and Shang-Keng Ma, Phys. Rev. **183**, 338 (1969).
[41]R. Abe and K. Aizu, Phys. Rev. **123**, 10 (1961); R. C. Clark, Proc. Phys. Soc. London **82**, 785 (1963); C. T. Schappert, Phys. Rev. **168**, 162 (1968).
[42]V. B. Shikin and Z. Veliev, Fiz. Nizk. Temp. **2**, 856 (1976) [Sov. J. Low Temp. Phys. **2**, 420 (1976)].
[43]A. C. Anderson, M. Kuchnir, and J. C. Wheatley, Phys. Rev. **168**, 261 (1968).
[44]I. M. Khalatnikov, Teoriya sverkthekuchesti (Theory of Superfluidity), Nauka, M., 1971, p. 238.
[45]a) F. Refi and L. Meyer, Phys. Rev. **119**, 1164 (1960); b) K. W. Schwarz, Phys. Rev. A **6**, 9158 (1972); c) B. A. Brody, P. D. Thesis, University of Michigan, 1970.
[46]R. M. Bowley, J. Phys. C **4**, 1645 (1971).

[47]R. G. Barrera and G. Baym, Phys. Rev. A **6**, 1558 (1972).
[48]B. D. Josephson and J. Lekner, Phys. Rev. Lett. **23**, 111 (1969).
[49]W. J. Glaberson and W. W. Johnson, J. Low Temp. Phys. **20**, 313 (1975).
[50]L. S. Reut and I. Z. Fisher, Zh. Eksp. Teor. Fiz. **60**, 1814 (1971) [Sov. Phys. JETP **33**, 981 (1971)].
[51]V. N. Bondarev, Pis'ma Zh. Eksp. Teor. Fiz. **18**, 693 (1973) [JETP Lett. **18**, 405 (1973)].
[52]A. V. Svidzinskiĭ, V. A. Slyusarev, and M. S. Strzhemechnyĭ, Trudy FTINT AN UkrSSR, FKS **5**, 23 (1973).
[53]a) A. J. Dahm and T. M. Sanders, J. Low Temp. Phys. 2, 199 (1970); b) M. Kuchnir, Ph. D. Thesis, University of Illinois, 1966; c) L. Meyer, H. T. Davis, S. A. Rice, and R. J. Donnelly, Phys. Rev. **126**, 1927 (1962).
[54]a) J. T Tough, W. D. McCormick, and J. G. Dash, Phys. Rev. **132**, 2372 (1963); R. D. Taylor and J. G. Dash, Phys. Rev. **126**, 1927 (1962). b) H. H. Tjerkstra, Physica (Utrecht) **18**, 853 (1952).
[55]K. O. Keshishev, Yu. Z. Kovdrya, L. P. Mazhov-Deglin, and A. I. Shal'nikov, Zh. Eksp. Teor. Fiz. **56**, 94 (1969) [Sov. Phys. JETP **29**, 53 (1969)].
[56]V. L. Ginzburg and L. P. Pitaevskiĭ, Zh. Eksp. Teor. Fiz. **34**, 1240 (1958) [Sov. Phys. JETP **7**, 858 (1958)].
[57]G. Ahlers and G. Camota, Phys. Lett. A **38**, 65 (1971).
[58]M. H. Coopersmith and H. E. Neustadter, Phys. Rev. **161**, 168 (1967); Phys. Rev. Lett. **23**, 585 (1969); T. P. Eggarter and M. H. Cohen, Phys. Rev. **25**, 807 (1970); **27**, 129 (1971); R. A. Young, Phys. Rev. A **1**, 983 (1970); J. P. Hernandez, Phys. Rev. A **5**, 635 (1972).
[59]V. B. Shikin, "Physics of condensed states," Trudy FTINT AN UkrSSR **25**, 80 (1973).
[60]V. B. Shikin, Yu. Z. Kovdrya, and A. S. Rybalko, *ibid.* **15**, 99 (1971).
[61]B. I. Shklovskiĭ and A. L. Éfros, Usp. Fiz. Nauk **117**, 401 (1975) [Sov. Phys. Usp. **19**, 137 (1976)].
[62]A. F. Andreev, Usp. Fiz. Nauk **118**, 251 (1976) [Sov. Phys. Usp. **19**, 137 (1976)].
[63]A. J. Dahm, Fiz. Nizk, Temp. **1**, 593 (1975) [Sov. J. Low Temp. Phys. **1**, 286 (1975)].
[64]K. O Keshishev and A. I. Shal'nikov, Fiz. Nizk. Temp. **1**, 590 (1975) [Sov. J. Low Temp. Phys. **1**, 285 (1975)]; K. O. Keshishev, Author's Abstract of Candidate Thesis, IFP AN SSSR, M., 1976.
[65]V. N. Grigor'ev, B. N. Esel'son, and V. A. Mikheev, Zh. Eksp. Teor. Fiz. **66**, 321 (1974) [Sov. Phys. JETP **39**, 153 (1974)].
[66]J. D. Eshelby, "The continuum theory of dislocations," Advances in Solid State Physics, Vol. 3, Academic Press, 1956, p. 79; (Russ. Transl., IL, M., 1963). A. M. Kosevich, Osnovy mekhaniki kristallicheskoi reshetki (Fundamentals of Lattice Mechanics), Nauka, M., 1972.
[67]I. M. Lifshitz, Zh. Eksp. Teor. Fiz. **44**, 1349 (1963) [Sov. Phys. JETP **17**, 909 (1963)].
[68]A. F. Andreev and I. M. Lifshitz, Zh. Eksp. Teor. Fiz. **56**, 2057 (1969) [Sov. Phys. JETP **29**, 1107 (1969)].
[69]D. I. Pushkarov, Zh. Eksp. Teor. Fiz. **59**, 1755 (1970) [Sov. Phys. JETP **32**, 954 (1971)].
[70]V. P. Mineev, Zh. Eksp. Teor. Fiz. **63**, 1822 (1972) [Sov. Phys. JETP **36**, 964 (1973)].

Translated by S. Chomet